ACS Partner Journal
PRECISION CHEMISTRY
pubs.acs.org/PrecisionChem
Perspective

# Prospects for Tin-Containing Halide Perovskite Photovoltaics

Shuaifeng Hu,*,# Joel A. Smith,*,# Henry J. Snaith,* and Atsushi Wakamiya*

Cite This: *Precis. Chem.* 2023, 1, 69–82
Read Online
ACCESS | Metrics & More | Article Recommendations

**ABSTRACT:** Tin-containing metal halide perovskites have enormous potential as photovoltaics, both in narrow band gap mixed tin–lead materials for all-perovskite tandems and for lead-free perovskites. The introduction of Sn(II), however, has significant effects on the solution chemistry, crystallization, defect states, and other material properties in halide perovskites. In this perspective, we summarize the main hurdles for tin-containing perovskites and highlight successful attempts made by the community to overcome them. We discuss important research directions for the development of these materials and propose some approaches to achieve a unified understanding of Sn incorporation. We particularly focus on the discussion of charge carrier dynamics and nonradiative losses at the interfaces between perovskite and charge extraction layers in p-i-n cells. We hope these insights will aid the community to accelerate the development of high-performance, stable single-junction tin-containing perovskite solar cells and all-perovskite tandems.

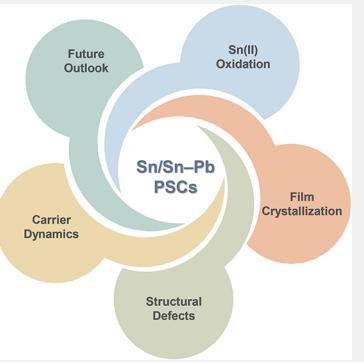


**KEYWORDS:** *solar cell, perovskite, tin, crystallization, surface chemistry, defect passivation, carrier dynamic*

## INTRODUCTION

Metal halide perovskites are unique materials, possessing ideal characteristics for photovoltaics: high absorption coefficients ($\sim 10^5$ $cm^{-1}$), tunable band gaps, and relatively benign defect populations.[1,2] Perovskite materials can be readily processed as thin films with low-cost solution- and vacuum-processing fabrication routes and integrated into photovoltaic (PV) devices, termed perovskite solar cells (PSCs).

Over the past decade, the power conversion efficiency (PCE) of single-junction PSCs has surpassed 25%, for devices fabricated in both n-i-p (regular)[3] and p-i-n (inverted)[4] structures, on par with state-of-the-art crystalline silicon solar cells.[5,6] Further improvements to the efficiency of single-junction devices will become increasingly difficult as the field approaches the radiative efficiency limit. Tandem solar cells[7] made by combining several absorbing layers in one device configuration offer a promising route to surpass the radiative efficiency limit for single-junction solar cells, increasing from 33% to 45% for tandems in an idealized theoretical scenario.[8] When considering the total manufacturing costs to fabricate the cells, the most technoeconomically competitive devices are likely to be two-junction monolithic tandems[9] that have a theoretical maximum efficiency of about 42% for the specific band gaps obtainable for metal halide perovskites.[10] For these cells, the wide band gap absorber layer is typically made with neat lead-based perovskites with a certain amount of $Br^-$ (bromide) ions at the X-site of the $ABX_3$ perovskite structure,[11] whereas the narrow gap subcells are typically conventional silicon (Si) or the Sn-containing metal halide perovskite materials.[10] Perovskite/Si tandems have recently been realized with an efficiency of 32.5%.[12] In close pursuit, perovskite/perovskite (all-perovskite) tandems have been achieved with current record efficiencies of over 29%.[13] Although this is lower than that of perovskite/Si, all-perovskite tandems employ much thinner absorber layers and move away from the energy-intensive production required for crystalline silicon, meaning that less energy-intensive production will be achievable at scale.[9,14] Efficiencies of over 30% are feasible for all-perovskite tandems with further optimization of the cell architecture and the quality of the wide- and narrow-gap subcells.[15] For realization of high-quality perovskites with narrow band gaps, alloying Sn and Pb (roughly half of each) at the B-site is currently the single accessible strategy. Owing to the band gap bowing effect,[16] mixed Sn–Pb perovskites exhibit a band gap of about 1.2 eV, lower than their neat-Sn- and Pb-based counterparts and the lowest possible for reported halide perovskites, making this the most optimal material for integration into all-perovskite two-terminal tandems.[7]

Although lead is abundant and sustainable and the toxicity impact when employed in PV modules is very low,[17−19] there is a desire to discover and develop perovskite PVs based on less toxic metals, for applications in consumer electronics, wearable PVs, and powering of biosafe devices.[20] Among the candidates, Sn-based perovskites are the most promising alternative,[21,22] with

**Received:** February 8, 2023
**Revised:** March 14, 2023
**Accepted:** April 3, 2023
**Published:** April 13, 2023





https://doi.org/10.1021/prechem.3c00018
*Precis. Chem.* 2023, 1, 69–82

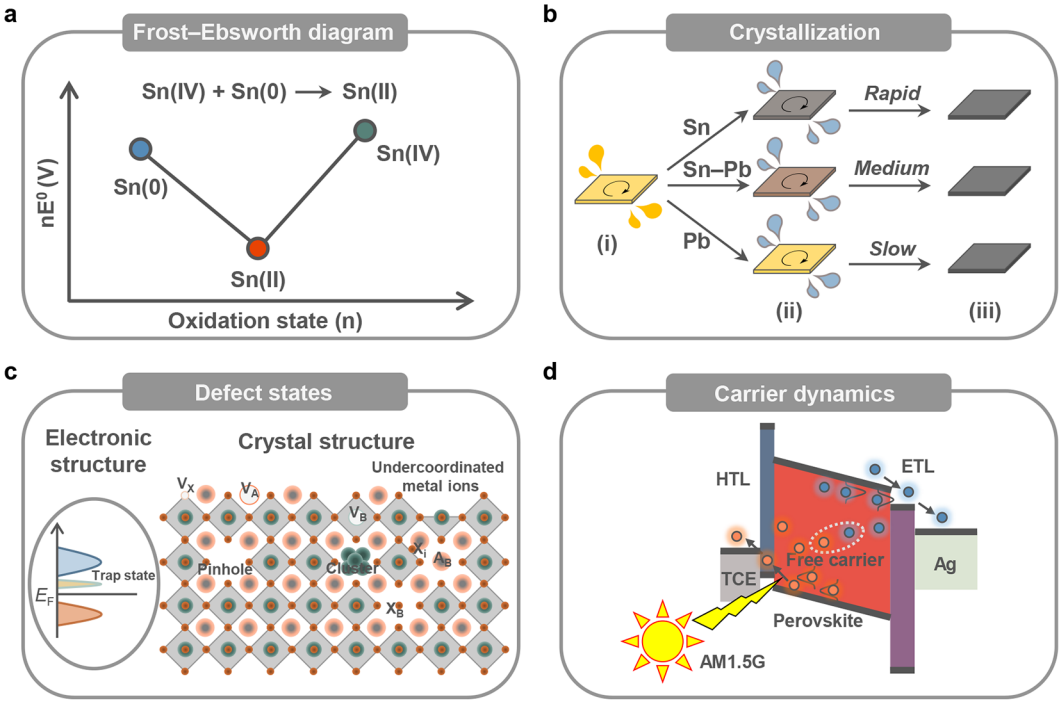


**Figure 1.** (a) Frost−Ebsworth diagram for Sn demonstrating the favorable comproportionation reaction between Sn(IV) and Sn(0) to form Sn(II). (b) Illustration of the crystallization of Sn-, mixed Sn−Pb-, and Pb-based perovskite films: (i) perovskite precursor solution coated on a substrate, (ii) films quenched with antisolvent, and (iii) final annealed films. Evolution of the color reflects the speed of crystallization. (c) Possible defect states in the perovskite structure. $E_F$ denotes Fermi level. $V_A$, $V_B$, and $V_X$ denote A-, B-, and X-site vacancy defects. $A_B$ and $X_B$ denote antisite defects where the B-site is substituted by an A-site cation or X-site anion, respectively. $X_i$ denotes a halide (X) at an interstitial site. (d) Illustration of carrier dynamics in PSCs with the p-i-n structure. TCE, transparent conducting electrode; HTL, hole-transport layer; ETL, electron-transport layer.

the PCE of neat-Sn perovskite solar cell devices approaching 15%.[21−25] The introduction of tin, however, raises several pressing issues for the perovskite films and consequently the corresponding solar cells:[26] for example, the instability caused by the facile oxidation of Sn(II) to Sn(IV), the substandard film quality associated with the rapid crystallization process, and accordingly the increased structural defect densities in the films.[27,28] All these drawbacks pose challenges that could hamper any potential advantages over neat-lead perovskites, considering that these neat-Sn perovskites have a band gap close to the ideal value, around 1.34 eV, that should result in the highest achievable efficiency for single-junction cells,[8] and the relatively high charge carrier mobility compared to that of the Pb analogues.[29,30]

In this perspective, we summarize the challenges for processing Sn-containing PSCs fabricated with the most studied and relevant compositions and highlight successful efforts made toward solving these individual issues; we also propose potential solutions and future research directions relating to each point. We hope that the insights presented can aid the community in realizing the next wave of Sn-containing PSCs with improved efficiency and durability.

## CHALLENGES AND SOLUTIONS FOR TIN-CONTAINING PEROVSKITE SOLAR CELLS

### Oxidation of Sn(II)

The preferred oxidation state of Pb is +2, where the Pb 6p orbital is involved in bonding and the outer s electrons are more tightly bound to the nucleus than the orbitals for the other group 14 elements because of the combined effects of relativistic contraction (particularly affecting s and p orbitals) and the 6s electrons being poorly shielded from the nuclear charge by 4d and 5f orbitals.[31] Without these effects, the two 5s electrons of Sn(II) are easier to lose with respect to the 6s electrons of Pb(II), leading to Sn(IV) being a slightly more stable oxidation state.[32] Consequently, for Sn-containing perovskite films, the required Sn(II) environment results in the notorious instability of these materials against external stimuli, especially oxygen. Given that, reducing agents and antioxidants are generally effective additives that reduce Sn(IV) in perovskite precursor solutions.

The reducing agent most widely used by the community is Sn(0) species in a powder[33] or nanoparticle[34] form, which reacts with Sn(IV) to generate Sn(II) via a comproportionation reaction (Figure 1a). In this way, the resulting solutions may also contain an amount of Sn(II) larger than that required for the designated stoichiometry, thus resulting in Sn-rich growth conditions, which could result in films with reduced Sn(II) vacancies. On the other hand, because the Sn(0) sources introduced have a small particle size, this approach generally leaves residual metallic Sn(0) in the resultant perovskite films, even when fabricated with finely filtered precursor solutions.[35] Metallic Sn(0) is a mild reducing agent, which may result in further adverse chemical reactions, or simply introduce morphological defects with larger area processing. Regarding tin-wire[35] and other organic reducing agents and antioxidants, we refer the reader to a comprehensive review from Cao and Yan,[27] with promising directions toward alternative additives without detrimental side effects.

$SnF_2$ has also been found to be indispensable for fabricating Sn-containing perovskite films with high quality and can prevent undesirable p-doping.[36,37] The fluoride ion is a hard Lewis base,


https://doi.org/10.1021/prechem.3c00018
Precis. Chem. 2023, 1, 69−82

so in solution it preferentially complexes to higher oxidation state Sn(IV) species, with the effect of converting $SnI_4$ to $SnF_4$, preventing Sn(IV) from being incorporated into the perovskite.[38] There are however several additional effects with $SnF_2$ addition. For instance, fluoride ions have been found to preferentially accumulate at the transport layer/perovskite interfaces,[37] and $SnF_2$ can cause secondary phases to form at the film surface,[39] which may lead to the undesirable effects on the cell performance. Although the optimal amount of $SnF_2$ for minimizing the background hole density may be as little as 1 mol %, based on the photophysical properties of the films,[40] in films used for efficient PSCs, $SnF_2$ addition is typically about 10 mol % with respect to the total Sn(II) content. Variability in secondary-phase behavior has been observed as dependent on the A-site and metal composition;[41] therefore, the optimal $SnF_2$ loading for ideal optoelectronic performance of a particular stoichiometry is necessary. Further understanding of the chemistry of fluoride and other halide additives in Sn-containing precursor solutions, and decoupling this from the concomitant effects of Sn-rich growth conditions,[42] could accelerate the development of alternatives that can outperform $SnF_2$.

For additives that do not incorporate into the perovskite phase, most are bulky and inhibit moisture or oxygen ingress, providing the films with a substantially improved ability to withstand oxidation, which is initiated—and most likely remains concentrated—at grain surfaces rather than in the perovskite bulk.[43,44] In particular, this can be by reducing the "dimensionality" of the perovskite from a continuous $ABX_3$ corner-sharing structure (3D) by the insertion of organic cations in a spacer layer that are too large to fit within the A-site perovskite cage.[45−47] Forming such 2D or quasi-2D materials, or surrounding the 3D perovskite with such phases,[48,49] is an effective strategy to enhance the durability of the perovskite against external stimuli[50] while maintaining or even improving the efficiency of photovoltaic devices further.[23,24,51]

Alternatively, varying the chemical composition of the perovskite phase itself by alloying may create a greater ability to mitigate oxidation as it could change the chemical surroundings of the active center to make it energetically less vulnerable. For example, in comparison to that of neat-Sn perovskites, the degradation is greatly hindered when Sn is blended with Pb to form mixed Sn−Pb perovskite materials, increasing the oxidation reaction activation energy and slowing down the kinetic process.[52,53] For mixed Sn−Pb perovskites specifically, air exposure is thought to result predominantly in the formation of deep trap states, rather than the significant electronic doping generally observed in neat-Sn perovskites.[53] This could be related to the energetic alignment of the same defect state(s), or the propensity for different defects to form depending on the composition.[42,54] Doping the material with Ag(II), which has a six-coordinate ionic radius (1.15 Å) close to that of Sn(II) and Pb(II), was found to be effective for suppressing the oxidation of mixed Sn−Pb perovskite films.[55] The effectiveness of different metal-ion-doping strategies has been examined and proposed for both the A-[56] and B-site[42,57,58] cations. Additionally, as with Pb, accidental trace elemental doping is not broadly investigated in the community and may have undesirable effects. Many doping strategies developed in mixed Sn−Pb PSCs will also be applicable to neat-Sn PSCs and vice versa, considering the underlying mechanism of Sn(II) oxidation is analogous between these material systems. For this purpose, the ionic radius should be taken as a prerequisite condition for the choice of ions that can form a true alloy. Despite this, metal halide additives such as $ZnI_2$ (zinc iodide) have still shown benefits in mitigating oxidation, despite being too small to incorporate into the perovskite phase.[59]

Oxidation of Sn(II) triggered by the extra layers at the interfaces of the devices is another serious issue. The interfaces contain abundant active species that could potentially catalyze the oxidation process. Given the p-i-n cell as an example, both of the commonly used inorganic and organic hole-transport materials (HTMs), $NiO_X$ and PEDOT:PSS (poly(3,4-ethylenedioxythiophene):poly(styrenesulfonate)), could induce Sn(II) oxidation. The oxidation routes, however, are to some extent different. For $NiO_X$, depending on the processing route, redox-active oxygen and $Ni^{3+}$ species may be present at the surface and could potentially oxidize Sn(II) at this interface.[60] Some small molecules that adsorb or bind to the metal oxide, such as self-assembled monolayer (SAM) molecules, or desirable metal oxide species, like $GeO_2$ formed *in situ* at the interface,[61] could passivate interfacial traps and probably suppress redox reactions at the surface. For PEDOT:PSS, its acidity appears to catalyze the formation of $I_2$, which subsequently oxidizes Sn(II) to Sn(IV).[62] As $I_2$ is a common decomposition product of perovskites, preventing any phase degradation will be crucial to avoid this redox chemistry feedback loop.

The redox routes outlined are comparable among different potential sources of oxidation, and a more unified understanding of Sn(II) oxidation routes, including those in perovskite solutions, is gradually forming but still worthy of more investigation. For example, the interesting findings on Sn(II) oxidation by DMSO (dimethyl sulfoxide), a near-ubiquitous solvent in the precursor solution of Sn-containing perovskite films, provides remarkable insight for further study. It was revealed that, under the film-processing temperature, hydroiodic acid can catalyze a redox reaction between the DMSO and Sn(II), resulting in $SnI_2$ to $SnI_4$, with additional effects on the organics present in solution.[63,64]

All of these routes lead to imperfect materials and accordingly reduce the efficiency of Sn-containing PSCs. Alternative strategies, such as modified PEDOT/PEDOT-free HTLs/SAM-based HTLs (HTL denotes hole-transport layer),[62,65−67] surface/interface postmodification,[25,41,68] DMSO-free[69] or solvent-free[70,71] processing systems, and material encapsulation techniques,[72] that efficiently work for Sn-containing perovskites are thus a pressing area for reducing the effect of Sn(II) oxidation in perovskites.

## Crystallization of the Films

The differences in chemistry between Sn(II) and Pb(II) have stark effects on the crystallization of Sn-containing perovskite phases. This is immediately evident by the faster reaction rate of $SnI_2$ with MAI (methylammonium iodide) or FAI (formamidinium iodide) compared to that of $PbI_2$, which affects the nucleation and growth rate of Sn perovskites during the film formation process (Figure 1b).[32,73,74] Both Sn and mixed Sn−Pb materials are consequently able to crystallize from solution at room temperature,[75,76] which necessitates better control over the formation process to avoid poor crystallinity. Control over crystallization in Sn perovskites has been achieved via many strategies, which are comprehensively covered for neat-Sn compositions in recent reviews.[77,78] Here we outline research highlights as well as the key differences and challenges compared to neat-Pb compositions.


https://doi.org/10.1021/prechem.3c00018
Precis. Chem. 2023, 1, 69−82

For solution processing, to understand crystallization we must begin in the liquid state, where perovskite solutions contain colloidal particles. Reported dynamic light scattering (DLS) measurements on Sn-containing solutions show up to three different size populations of particles, and in some cases the largest colloids or agglomerates present in solution are significantly larger than those for neat Pb.[79−83] The size distribution of the larger particles is also affected somewhat inversely to the behavior in Pb perovskites, where the addition of acid leads to a reduction in colloid size through reaction with DMF (dimethylformamide).[84] In current reports the addition of acids,[79] bases,[80] diammoniums,[83] or chloride salts,[81,85] all seemingly increasing the average size of the large particles in Sn-containing perovskites. With use of small-angle X-ray scattering, which is a more direct measure of size distributions in films than DLS,[86] small nanometer-size colloids are confirmed to be present in $FASnI_3$, as have been observed directly in neat-Pb perovskites,[87] along with larger species. Notably, when the DMSO solvent is exchanged for DMF, and in conjunction with $SnF_2$, these larger species are no longer evident, and the presence of the smaller colloids are more pronounced.

As with Pb, solvents and halides coordinate to Sn and are in competition. Absorption spectroscopy on Pb solutions has revealed more highly coordinating solvents inhibit the formation of higher valency solvated polyiodide plumbates ($PbI_m^{2-m+}$).[88] These may exist as isolated complexes, as bridged chains, or within the colloidal species.[88,89] Moving to strongly coordinating halide ligands ($Cl^- > Br^- > I^-$), the absorption from more highly valent polyhalide plumbates is reduced.[90] As there are few reports presenting absorption spectra of Sn perovskite solutions, and most being only $SnI_2$,[82,91,92] the effect of solvents and halides on halogenostannate complexes ($SnX_m^{2-m+}$) in solution is yet to be understood, although undoubtedly impacts the crystallization.

As yet, there are few reports on the intermediate crystallization pathway, with to the best of our knowledge no solvate crystal structures reported containing organic cations or deviating from $SnI_2{\cdot}n$(solvent) stoichiometry, other than with bidentate ligands.[41] Possible relevant intermediates so far reported are all $SnX_2$ solvate phases, $SnI_2{\cdot}$DMSO,[23] $SnI_2{\cdot}$2DMSO,[93] $SnI_2{\cdot}$3DMSO,[94] $SnI_2{\cdot}$DMF, and $3(SnI_2){\cdot}$2DMF as well as solvates with Br, Cl, and F.[93] Although $PbI_2{\cdot}$solvate phases generally adopt $NH_4CdCl_3$-type 1D structures with edge-sharing six-coordinate holodirected octahedra,[95,96] the coordination geometries of $SnX_2$ solvates are generally hemidirected.[97] In comparison to Pb, this is likely due to the higher stereochemical activity resulting from interactions between the Sn 5s antibonding orbital and donor orbitals.[98,99] Similarly, the O−Sn bond lengths are shorter in $SnI_2{\cdot}n$(solvent) than for $PbI_2{\cdot}n$(solvent), and the strength of the coordinating bond of DMSO to Sn is stronger than that to Pb. Beyond solvate intermediates, the widely known polytype phases with Pb[100] have not been reported for Sn with $FA^+$ cations.[101,102] Despite this, several studies do show XRD data from intermediate phases, which do not match the reported structures.[85,101,103] Few reports have investigated the crystallization pathway via *in situ* methods,[76] so further study is required to confirm the nature of these potential phases and their impact on crystal quality. This could be supported by a clearer understanding of the degradation products from Sn-containing perovskites.

In common with Pb, almost all reported devices utilize thin films processed by antisolvent quenching the perovskite precursor film with a solvent orthogonal to the primary solvents (typically chlorobenzene, anisole, or toluene).[104] This can be avoided, for example, through gas quenching,[105] which necessitates finer process control but is ultimately closer to a viable industrial process, or vacuum annealing.[92] Alternatively, options include two-step processes where the organohalide is coated onto a metal halide template,[103,106] or the use of alternative solvent systems such as ionic liquids.[107,108] Both of these approaches constitute substantially alternative crystallization pathways that will consequently affect the crystal quality and defect formation. More varied efforts to alter the crystallization route for Sn-containing perovskites could yield significant advances in material quality. Similarly, thermal evaporation has huge potential for commercially relevant perovskite deposition,[70,71] despite relatively few reports at present. This is likely because of the necessity for dedicated Sn or mixed Sn−Pb evaporation chambers to avoid trace Sn contamination, which in neat-Pb materials can have a deleterious effect on the optoelectronic quality of the material.[40,109] A drawback, however, is the more limited range of evaporable materials and consequently additive approaches that can be employed.

Beyond $SnF_2$ discussed above and other Sn halides, additive engineering to alter Sn-perovskite crystallization has been used across a vast array of compounds,[78] from pseudohalides such as $SCN^-$ (e.g., $NH_4SCN$,[110] $Pb(SCN)_2$[109]) to amino acids,[81] along with a variety of other acids and bases.[80] Although it is understood that these can alter the colloidal chemistry, nucleation, and growth, a unified understanding of the effect of different functional groups or ions specific to Sn-containing materials has yet to be realized. For example, amino acids have proven to be very effective at improving the performance of mixed Sn−Pb PSCs,[81] suggesting great potential for further study. Alloying "small" cations (such as guanidinium,[111] ethylammonium, and ethylenediammonium[112]) has also yielded enhancements in performance. Several of the highest efficiencies for $FASnI_3$ (>14%) have come through the addition of bulky ammonium halide additives, commonly used as spacers in 2D phases.[23,24] These result in highly oriented films; however, much as with thermal degradation of methylammonium,[113] other alkylammoniums may suffer from thermally induced chemical decomposition or reorganization in films.[114] Orientation and high efficiencies have also been achieved by the use of FACl (formamidinium chloride),[25] mirroring the widely used MACl (methylammonium chloride) additive in $FAPbI_3$.[115] It remains unclear, as with Pb perovskites, if orientation is itself beneficial for performance, or whether this is an outcome of better controlled growth, bicontinuous grain structure between charge extraction layers, and/or facet control at the top surface, which may enable more precise control over surface defect states.[116]

## Defect States in the Films

The rapid crystallization process leads to the formation of abundant imperfections initially present in Sn-containing perovskite films. In addition, the vulnerable nature of the films, especially to the effect of external stimuli, leads to films having a high probability of forming defects. In general, defects in the films can be classified with dimension, that is, 0D to 3D defects.[117] Zero-dimensional defects (point defects) include interstitial, vacancy, and substitutional defects. One-dimensional defects are linear defects such as edge or screw dislocations. Two-dimensional planar defects include stacking faults and grain boundaries, whereas 3D defects are in the form of pinholes, cracks, precipitates, and impurities.[28] Electronically, any of these


https://doi.org/10.1021/prechem.3c00018
Precis. Chem. 2023, 1, 69−82

defects that introduce new energetic states within the band gap of the primary phase can also be described in terms of the trap state they introduce: "shallow" for states close to a band edge and "deep" defects that are toward the middle of the band gap (Figure 1c).[118,119] These can be directly introduced trap states within the primary phase, or other defects can also introduce trap states—such as in secondary phases or interfaces with a secondary phase—all of which may be nonradiative recombination pathways, with deep traps being the most problematic.[120]

For $ASnI_3$ perovskite films, the point defects with the lowest formation energy are generally calculated to be tin vacancies ($V_{Sn}$), with variation dependent on the cation and growth stoichiometry conditions.[42,121−123] Luckily, this is thought to not introduce a deep level trap state; however, the facile formation of $V_{Sn}$ is reflected in the stability of the material. Given the facile formation of $V_{Sn}$ or loss during degradation of Sn(II),[124] halide interstitials ($X_I$), antisite substitutions ($A_{Sn}$ and $X_{Sn}$), and undercoordinated $I^-$ ions are point defects that could more readily form, particularly under Sn(II)-deficient conditions. Depending on the composition, these defects may constitute deep level traps in the perovskite films, which will increase nonradiative recombination.[28,42] Note that the surface of the perovskite films is prone to interact with the external reactive species such as $H_2O$ and $O_2$,[125] leading to the accelerated degradation and mass loss of the materials. Therefore, stabilizing exposed surface sites where these defects are more likely to form and suppressing the movement of the ions in the perovskite should be able to reduce the formation of deep level traps. Coordinating or adsorbed molecules, such as Lewis acids/bases, could help in this aspect, as they likely create some covalent bond and/or electrostatic interactions with these defects.[126] In particular, zwitterions would be particularly worthy of further study for defect passivation, as their combination of positive and negative functional groups may enable simultaneous passivation of defects with either charge. Intriguingly, in mixed Sn−Pb perovskites, we recently found that $V_I$ (iodide vacancies) formed in mixed Sn−Pb films will mostly be at Sn rather than at Pb centers, as the formation energy at these sites is more favorable.[127] Accordingly, when passivation strategies are applied, targeting Sn-based defects selectively for passivation in films is desirable.

Defects with higher dimensions sometimes form with the accumulation and transformation of those of lower dimension. Thus, to some extent, reducing the formation of point defects may also accordingly reduce the density of extended defects. The formation of high-dimensional defects is more directly associated with the film crystallization process. Thus, exploring approaches that are able to manipulate the crystallization route to form films with reduced grain boundaries, reduced stacking faults, better homogeneity, and a lower concentration of impurity phases is essential, as discussed above. Further fundamental study of the effect of secondary phases, inclusions, and twin boundaries in Sn-containing perovskites, mirroring work on Pb perovskites,[128−130] would be highly useful in this regard.

Considering that the defect formation and material degradation is largely initiated at and dominated by exposed sites,[43] that is, the surfaces and grain boundaries, these locations should take priority when conceiving of passivation strategies. Given the different populations of defects that can form and the tendency for p-type charge transport,[131,132] particular attention must be paid to passivating electron traps. This is most critical at the top surface in p-i-n devices where the perovskite/ETL interface is located.

## Charge Carrier Dynamics and Energy Level Matching

The defects discussed above will accordingly affect the charge carrier dynamics in solar cells by forming states that can trap carriers (Figure 1d). Carrier diffusion lengths must be long enough to reach the interfaces that make contact with the extraction layers in the cells. Once the carrier lifetime is sufficiently long, thereafter, efficient extraction is indispensable for realizing efficient cells. Additionally, for Sn-containing PSCs, similar to Pb perovskites, charge carrier extraction will be modulated by mobile ions, which can induce hysteresis effects in photovoltaic device measurements.[132−134] These mobile ions can induce instability through a variety of redox reactions discussed earlier, as well as migrating into transport layers such as fullerenes, further altering the interface energetics.[135] Reaching a complete understanding of the effects of mobile ions and the effects they have on device performance requires further study; however, it has been suggested that ion migration may be less severe in mixed Sn−Pb perovskites than neat Pb since the activation energy for ion migration could be relatively higher.[135,136]

The highest efficiencies for Sn-containing PSCs are generally obtained with the p-i-n cell structure.[27,81,102] This is because, first, the energy level alignment at the interfaces of the perovskite and charge-transport layers in p-i-n cells is better than that in n-i-p cells;[22] second, HTL dopants[137] and ETLs such as $TiO_2$[138] employed for n-i-p cells will react more readily with the perovskite, causing damage to the films. However, in our experience, Sn PSCs in the n-i-p configuration generally demonstrate higher output current than those in the p-i-n configuration, most likely because (in cases where the perovskite is p-type) the minority carriers are generated close to the incident light side where they can be more easily extracted, even with short diffusion lengths. Therefore, manipulating the carrier dynamics and developing charge-transport materials and interfaces that minimize losses by having energy levels well-aligned to the perovskite, together with no detrimental chemical reactivity, could result in n-i-p cells with efficiencies at least comparable to those in p-i-n cells. Although unbalanced carrier conductivities due to p-doping may limit the photovoltaic performance compared to an intrinsic absorber layer in the same architecture, there are some applications where this could be desirable, for example, transistors.[132,139,140]

Because p-i-n cells account for the vast majority of high-efficiency reports, and for the current advantages outlined above, we mainly focus on a discussion of this architecture. Current reports almost entirely employ Cu (copper) or Ag (silver) as the back contact in this architecture, which is problematic for stability in conjunction with mobile ions, for example, resulting in AgI (silver iodide) formation. Ways to mitigate this could be by inhibiting contact between $I^-$ and Ag or replacing the metal electrode with less redox active materials such as carbon. Notably, the most stable low gap perovskite cells reported to date employ an $SnO_2$ buffer layer and a sputter-coated transparent conducting oxide (TCO) top contact.[141] Regarding metal oxide interface-induced degradation, this can be greatly suppressed by modification with SAM molecules, which can work both as buried interface passivation and as a charge-selective contact. In Pb perovskites, hole-selective SAMs are outperforming conventional polymer or metal oxide HTLs; in the best performing carbazole derivative SAMs most likely by


https://doi.org/10.1021/prechem.3c00018
Precis. Chem. 2023, 1, 69−82

reducing the interfacial electron trap density and by efficiently transferring holes into the TCO contact.[142,143] However, the best SAMs currently developed perform less efficiently for Sn-containing PSCs, as evident from the limited successful attempts.[144,145] There are several reasons for this: first, the unsuitable energy level alignment. The reported 2PACz and Me-4PACz carbazole SAMs have HOMO levels around −5.6 to −5.9 eV.[142,146] This is deeper than the VBM of Sn PSCs, nominally around −5.20 to −5.4 eV,[29,147] or even shallower in some mixed dimensional compositions.[51] This is much shallower than that for neat Pb where the valence band is formed from orbital hybridization between I 5p and (deeper) Pb 6s orbitals, rather than (shallower) Sn 5s in neat Sn and mixed Sn−Pb perovskites.[16] Therefore, tuning the work function of the SAM-based contact by mixing SAM molecules with different energy levels[148] and/or developing new SAMs with energetics better tuned to Sn-containing PSCs[149] are directions worthy of exploration. Second, an issue may be poor coverage of the SAMs on the TCO substrate. With other transport materials, this can lead to current leakage in devices through the loss of shunt resistance due to the perovskite contacting the TCO directly. If the impacts of this are more severe in Sn-containing perovskites, this could be due to higher hole conductivity (if p-type), causing shunt pathways to be more detrimental, or generally poor processing tolerance of the Sn-based perovskite films affecting the crystallinity at this interface. To mitigate this if this is an issue, improving the quantity of SAM molecules binding to the TCO substrate is critical. Improving the SAM coverage could be realized by, for example, increasing the active −OH groups at the TCO substrate surface, as this would increase the sites that are able to react with the proton(s) from the terminal group of the SAM molecules, usually $-PO(OH)_2$ and −COOH. Therefore, developing new SAM molecules that promise more suitable energy level alignment and/or improved coverage on the metal oxide electrode is key to release the potential of SAM-based charge-selective contacts that have proven so successful for Pb PSCs. Regarding this, adding additional small phosphonic acid molecules that can bind to metal oxide surface sites that have not been coated by the primary SAM molecules has proven effective for Sn-containing PSCs.[145] Furthermore, new SAM molecules with multiple phosphonic acid anchoring groups that would bind more strongly and allow control of the molecular orientation of the SAM on the metal oxide surface would be an effective way to realize well-performing SAM-based Sn-containing PSCs.[150]

Beyond the already problematic reproducibility of Sn-containing PSCs, in our experience consistent fabrication on SAMs with the quality that meets the requirement of Sn-containing perovskite films is even more challenging. Further understanding of how the final SAM/TCO contact is affected by the layer processing, for example, the concentration of the SAM solution, solvent, annealing temperature, and surface state of the TCO substrate etc., is more critical than that for Pb compositions. In addition, the currently employed additive mixtures may be optimized for PEDOT:PSS, and the requirements on SAM layers may be different. $FASnI_3$ specifically has been shown to form an interfacial SnS (tin sulfide) phase at the buried interface with PEDOT:PSS, which was not observed for mixed Sn−Pb, but other beneficial reactivity may occur.[151]

Besides the HTL, the ETL interface is also critical in determining the performance of PSCs, particularly the $V_{OC}$. For Sn-containing PSCs, the most common ETLs are the fullerenes $C_{60}$ and PCBM (phenyl-$C_{61}$-butyric acid methyl ester), owing to their good conductivity and reasonable alignment. For facile processing, thermal evaporation can be used for $C_{60}$, enabling fine control over the film thickness, conformality, and homogeneity. On the other hand, it is thought to introduce deep trap states when in direct contact with the perovskite, which can cause severe interfacial losses, even within the first monolayer.[152] One approach to mitigate this is using an interlayer inserted between the perovskite and the $C_{60}$ layer to avoid their direct contact and suppress interfacial losses. For example, fullerene derivatives, such as $C_{60}$ pyrrolidine tris-acid (CPTA)[127] and fullerene-*n*-butyl-pyridine,[153] would reduce the interfacial recombination caused by the $C_{60}$ ETL, thanks to their apparent ability to bind to undercoordinated metal centers while maintaining efficient electron transport. Accordingly, for maximizing the efficacy of the inserted interlayer, both passivation and carrier transporting characteristics may be the criteria that need to be fulfilled.

Regarding the interfacial loss, energy level matching between perovskite films and charge-transport layers is also key to unleashing the efficiency potential of Sn-containing PSCs, as the materials optimized for Pb perovskites may be less suited to their shallower energy levels.[29] For example, mixed 2D/3D Sn perovskite films with a phenethylammonium ($PEA^+$) spacer have a conduction band minimum of −3.69 eV,[51] resulting in a large energy level offset between the conventional $C_{60}$ ETL, with the LUMO level of −4.21 eV.[34] Fullerene bisadducts, for example, indene-$C_{60}$ bisadduct[51] and diethylmalonate-$C_{60}$ bisadduct,[154] can reduce the energy offset as they exhibit shallower LUMO levels compared to $C_{60}$. However, processing high-quality fullerene ETLs is quite challenging, as the weak intermolecular forces between the fullerenes can result in a variety of packing arrangements and disorder.[155] Energetic disorder in this layer may result in density of states broadening and less defined band edge or midgap states, both of which result in a reduction of the quasi-Fermi level splitting and thus voltage loss in PSCs. It may be possible to mitigate these effects through a better understanding and control of the packing of these ETLs.[156,157] This could be achieved by optimizing the processing solvent and/or temperature during the annealing process, resulting in a high degree of molecular ordering and consequently minimal energetic disorder.[158] Alternatively, molecular ordering of the fullerene layer could be controlled by functionalization, targeting molecules with specific terminal groups that would chemically interact, bind, or even chelate to metal centers in the perovskite underneath.[159] More generally, developing alternative fullerene or nonfullerene ETLs that are well-matched to the Sn-containing perovskite conduction band together with acceptable conductivity should lead to reduced interfacial losses.

From the perovskite side, interfacial recombination can also be suppressed by modifying the perovskite surface. For the top exposed surface in the p-i-n cell, post-treatment is an efficient and direct way to tune surface defects. In general, molecules applied for this purpose contain ammonium and/or amine functionalized units, thanks to their differing interactions with the perovskite films being modified. For the ammonium-based treatments, electrostatic interactions enable $-NH_3^+$ terminal groups to reside at the A-site of the perovskite surface. On the other hand, the amines, $-NH_2$, have different potential reactions, such as reacting with organics (primarily $FA^+$)[4,160] or potentially coordinating to exposed metal sites via the lone pair. For p-i-n cells, an n-type top surface would theoretically reduce the trapping of the photogenerated electrons, reduce the


https://doi.org/10.1021/prechem.3c00018
Precis. Chem. 2023, 1, 69−82

hole density at the surface, and enable efficient charge transfer at the ETL interface, thus suppressing nonradiative charge carrier recombination. Specifically, an n-type surface can be realized with both small diammonium cations and diamines, that is, ethylenediammonium ($EDA^{2+}$)[81,161] /1,3-propane diammonium ($PDA^{2+}$)[162] /piperazinium ($PP^{2+}$),[163] and ethylenediamine[164,165] /piperazine,[127] despite different proposed mechanisms. However, primary ammoniums like butylammonium ($BA^{+}$)[162] have mostly proven ineffective for p-i-n cells including mixed Sn−Pb and Sn materials.

For linear diammonium cations, the length of the alkyl chain can alter the dimensionality of compounds that can form. For iodide-dominated perovskite compositions, $EDA^{2+}$ and $PDA^{2+}$ cations cannot act as a spacer to form 2D layered materials.[47] In contrast, when diammonium cations with size greater than or equal to 1,4-butane-diammonium ($BDA^{2+}$), a Dion-Jacobson phase perovskite can form.[46] The potential to form different dimensionality phases that will drastically alter the electronic properties at the surface must be considered when interpreting the effect of different modifications. Since the small linear diammoniums $EDA^{2+}$ and $PDA^{2+}$ are unable to form 2D phases, they can instead enable different kinds of surface regulation. We have proposed with $EDA^{2+}$ that electrostatic interactions force one ammonium group to sit at the A-site of the perovskite structure with the other facing out of the film surface.[81] The stereochemistry with the longer chain $PDA^{2+}$ perhaps means this does not occur, so if the passivation is indeed similar, then further investigation of the precise mechanism is needed. The likely origin of the performance enhancement is through n-doping or tuning of the surface dipole that will reduce the hole density at the interface and inhibit nonradiative recombination between the perovskite and ETL.[81,161] If confirmed, this would be analogous to the mechanism of field effect passivation by LiF (lithium fluoride), a widely used interlayer that can enhance the perovskite/$C_{60}$ interface.[166]

Back to the neutral diamines, the active lone pairs will modify the surface through different routes. Thanks to the basicity of the diamine, they can potentially interact with the organic cation(s) at the perovskite surface or grain boundaries, that is, formamidinium ($FA^{+}$) and methylammonium ($MA^{+}$), with effects dependent on the diamine. For piperazine (PP), 4-aminopiperidine (4APP), and 4-(aminomethyl)piperidine (4AMP), this is thought to be by scavenging protons from the cations.[127] In these cases, the working mechanism of the diamine treatments is likely comparable to the diammoniums, but with any additional effects caused by the deprotonation of A-site cations. Alternatively, for other amines, amine-$FA^{+}$ condensation reactions expelling ammonia can take place, as first identified for methylamine (MA) in solution.[160] This could happen at the surface, such as when modified with 3-(aminomethyl)pyridine (3-APy),[4] and most likely ethylenediamine (EDA) and all other linear alkylamines.[160,167] In the case of 3-APy having the product $MPyFA^{+}$ (*N*-(3-methylpyridine) formamidinium), or for amine-$MA^{+}$, a simple transfer or sharing of acidic protons happens, forming $3APy^{+}$. The authors of this study propose the $MPyFA^{+}$ cation sites at the A-site of the perovskite, with the pyridine ring promoting the formation of positively charged $V_I$ (iodide vacancies), which act as shallow donors and induce a field that facilitates electron extraction. In one of the few reports showing some benefit with a primary ammonium treatment ($PEA^{+}$), this mechanism has also been proposed.[168] These top surface modifications seem to ensure less interfacial recombination, and accordingly better performance for the resultant cells, but further work is necessary to fully understand multiple concurrent, unusual effects. For example, the effect that some amines "polish" or "erode" the perovskite surface.[4,81,127]

Some approaches to top surface modification could also be applicable for modifying the buried interface. For example, targeted field engineering could also be achieved[169,170] by controlling the dipole on the substrate surface or perovskite buried surface to improve charge carrier extraction at the bottom interface. Alternatively, molecular passivation approaches might be possible to apply to the perovskite buried surface. Experimentally, it is more challenging to achieve these effects than with a top surface post-treatment, and could be implemented either by depositing a molecular layer on the substrate before the perovskite film or by adding it into the perovskite precursor solution. For the predeposition method, surface binding (analogous to SAMs) is necessary to prevent dissolution by the perovskite solvents. The alternative of introducing molecules in the precursor solution requires preferential accumulation at the bottom region of the films, for example, by using molecules that have chemical interaction with the substrate[171] and/or by engineering top-to-bottom heterogeneous crystallization of the perovskite.[172] Vacuum-based processing of the interfacial layer and/or perovskite (avoiding solvent redissolution) with precise layer thickness tuning might enable more precise control over this interface.

Interface modifications, irrespective of the charge-transport layer and/or perovskite films, are playing important roles for improving the interfacial charge carrier dynamics. In particular, the interesting *in situ* chemical reactions occurring between the neutral amines and the organic cation(s) of the precursor material offer huge potential for further exploration in PSCs and other perovskite-based electronics: highly targeted chemical reactions or surface species can be implemented into the perovskite system for specific aims.[167,173−176] In the end, we expect that most of the efficiency gains in Sn-containing PSCs will come through efficient management of charge carriers at the interfaces.

## Steps toward Commercialization

Regarding the sensitivity of Sn-containing perovskite films, there is a need to develop simple and universal protocols that have reasonable processing tolerances, along with a detailed reporting of methodologies, to avoid possible "hidden variables" that may be crucial for material quality. Doing this would facilitate more effective comparison of approaches invented in different laboratories to improve lab-to-lab reproducibility. This will accordingly lead to better reliability of the strategies when transferring to commercial environments.

With regards to stability, when Sn is incorporated, the development of effective encapsulation techniques is even more critical for the potential commercialization of this material.[141,177] Once encapsulation is sufficiently robust to eliminate extrinsic stressors (moisture, $O_2$), causes of intrinsic instability (heat, light, and electrical bias) are the most important areas to address as these will be experienced in operational conditions even with the best encapsulation. Understanding how the perovskite structure will decompose/react under these conditions is the most crucial area for future stability research across all compositions. To this end, removing volatile organic content from the perovskite (such as $MA^{+}$)[113] will likely be necessary. For mixed Sn−Pb PSCs, reducing the efficiency gap between MA-containing and MA-free cells will need significant further


https://doi.org/10.1021/prechem.3c00018
Precis. Chem. 2023, 1, 69−82

investigation,[66,67] especially on understanding/altering the crystallization dynamics.

Most commonly used solvents are toxic with damaging environmental impacts and therefore are heavily regulated in industry, so alternative less toxic solvent systems should be a priority for Sn perovskites, as with Pb.[178] Avoiding the usage of solvents can be achieved with vacuum-based film deposition protocols, that is, thermal evaporation, sputtering, and atomic layer deposition. For the perovskite layer, thermal evaporation has the advantages of minimizing dynamic variables in solution, reducing material consumption in terms of solvent waste, and enabling uniform, conformal deposition over large areas. This in turn allows for coating on textured and flexible substrates with ease. However, the vast majority of current research is directed to solution processing because of limited access to vacuum fabrication equipment and the challenges with thermal evaporation of Sn−Pb perovskites.[70,71] Direct industrial implementation of vacuum-processed films is expected in the coming years.[179]

Regarding the development of all-perovskite tandem solar cells, the strategies that have been developed for suppressing the voltage losses in single-junction solar cells can be directly incorporated into all-perovskite tandems. In particular, there are emerging parallels between passivation approaches for the ETL interface, which seem to be effective for both Sn-containing perovskites and ∼1.8 eV neat-lead perovskites, perhaps because of the similarities in the conduction band energies and ETL materials. For optimal tandem devices, reducing the current mismatch between the subcells is key.[180] Besides careful optimization of each band gap, increasing the absorption of the narrow-gap mixed Sn−Pb junction, especially in the near-infrared (NIR) region, will be beneficial. This could be realized by increasing the thickness of the films, reducing the parasitic absorption of the interconnecting layer, or introducing reflective or light-trapping nanostructures at the back contact to increase photon absorption. Alternatively, this may include consideration of bifacial all-perovskite tandem solar cells with transparent back contacts.[62,181,182] As well as harvesting additional albedo intensity to increase the energy yield, this could also decrease the optimal band gap of the wide gap junction. This would also reduce the necessary incorporation of $Br^-$ ions at the X-site for the wide gap material, making higher efficiencies and stability easier to achieve, together with reduced halide segregation and interfacial losses. Bifacial configurations may be preferred industrially in the long term, with bifacial modules expected to account for a 55% share of the global PV market by 2031.[180] In addition, developing interconnecting layers that have good vertical conductivity with maximized horizontal resistance to mitigate shunt pathways, as well as high NIR transmittance, is also key to minimizing losses in the tandem cells and the optical loss for the narrow-gap mixed Sn−Pb perovskite rear absorber.

## CONCLUSIONS AND OUTLOOK

In this perspective, we have outlined critical issues for further development of Sn-containing PSCs and provided some potential strategies toward each. In general, the facile oxidation of Sn(II) and reactivity of Sn-containing perovskite films is the first issue to be addressed by all laboratories in the field. This leads to irreproducibility and poor material quality, severely impacting the efficiency and stability of cells. Improving the understanding of Sn(II) oxidation and other degradation pathways in the perovskite system, as well as finding the most effective ways to mitigate these effects, will require more efforts by the community, both experimentally and computationally. The film crystallization routes of Sn-containing perovskites, which differ from Pb-based materials, are still yet to be understood fully. More research on understanding the solution chemistry and the role of different additives, especially using *in situ* measurements, will guide the design of the materials and the optimization of cell fabrication processes. However, a global picture of how the molecules affect the precursor solution stage and how this affects the following crystallization process, and their impacts on defect states and improved carrier dynamics in cells, is mostly lacking. Beyond solution processing, the development of vacuum-based methods for film growth must continue to be explored. Modifying the perovskite surface is critical to carrier extraction at the interfaces of PSCs but relies on a detailed understanding of the complex surface chemistry with many potential avenues of study. In parallel, improving the stability of Sn-containing perovskites is key to realizing their practical application. This will require a deeper scientific understanding of the origins of instability as well as advancement of the techniques to realize robust passivation and encapsulation methods. With continued research of the chemistry of Sn(II) oxidation, crystallization, defect characteristics, and electronic properties of films, the reproducibility and precise control over fabrication of efficient and stable Sn-containing PSCs can be achieved.

## AUTHOR INFORMATION


### Corresponding Authors

**Shuaifeng Hu** − *Institute for Chemical Research, Kyoto University, Kyoto 611-0011, Japan;* orcid.org/0000-0003-1312-075X; Email: shuaifenghu@yahoo.com

**Joel A. Smith** − *Clarendon Laboratory, Department of Physics, University of Oxford, Oxford OX1 3PU, U.K.;* orcid.org/0000-0001-6889-4408; Email: joel.smith@physics.ox.ac.uk

**Henry J. Snaith** − *Clarendon Laboratory, Department of Physics, University of Oxford, Oxford OX1 3PU, U.K.;* orcid.org/0000-0001-8511-790X; Email: henry.snaith@physics.ox.ac.uk

**Atsushi Wakamiya** − *Institute for Chemical Research, Kyoto University, Kyoto 611-0011, Japan;* orcid.org/0000-0003-1430-0947; Email: wakamiya@scl.kyoto-u.ac.jp

Complete contact information is available at: https://pubs.acs.org/10.1021/prechem.3c00018

### Author Contributions

#S.H. and J.A.S. contributed equally to this work.


### Notes

The authors declare the following competing financial interest(s): H. J. S. is co-founder and CSO of Oxford PV Ltd. and Helio Display Materials Ltd. A.W. is co-founder and CSO of Enecoat Technologies Co., Ltd.

### Biographies

Shuaifeng Hu is a Ph.D. candidate in the Department of Chemistry, Graduate School of Science of Kyoto University in Japan. His research focuses on fabricating well-performing p-i-n perovskite solar cells with particular interest in narrow-gap mixed Sn−Pb perovskite solar cells and perovskite-containing tandems.

Joel A. Smith is a postdoctoral researcher in the Department of Physics, University of Oxford, Oxford, UK. His research focuses on the development of metal halide perovskites for use in single-junction and

tandem solar cells. Specifically, he is interested in understanding and developing novel crystallization approaches and solution chemistries to enable scalable processing of perovskites. He has particular expertise with lab- and synchrotron-based 2D X-ray diffraction as well as *in situ* measurements to understand the phase behavior and stability of these materials.

Henry J. Snaith is the Binks Professor of Renewable Energy in the Department of Physics, University of Oxford, Oxford, UK. His research focuses on developing and understanding new materials and device concepts for photovoltaic solar energy conversion. His research group works with organic, metal oxide, and metal halide perovskite semiconductors, processed via solution- or vapor-phase deposition methods. His interdisciplinary work includes new material synthesis and discovery, device fabrication and development, advanced characterization methodologies, and theoretical modeling. Beyond his academic appointment, Henry Snaith is also a cofounder and CSO of two spinout companies, Oxford PV Ltd. and Helio Display Materials Ltd., commercializing metal halide perovskites for PV and light-emitting applications, respectively.

Atsushi Wakamiya is a professor in the Institute for Chemical Research of Kyoto University in Japan. His research focuses on the design of novel function materials that are applicable for making efficient and reliable perovskite solar cells and the development of the fabrication strategies for perovskite solar modules and flexible lightweight perovskite solar cells.

## ■ ACKNOWLEDGMENTS

This work was supported by JST-Mirai Program (JPMJMI22E2), NEDO, International Collaborative Research Program of ICR, Kyoto University, JSPS for a Research Fellowship for Young Scientists (21J14762), the China Scholarship Council (CSC), the UK Engineering and Physical Sciences Research Council (EPSRC) under projects EP/V027131/1 and EP/S516119/1 and the US Office of Naval Research (ONR) under award number N00014-20-1-2587.

## ■ REFERENCES

(1) Green, M. A.; Ho-Baillie, A.; Snaith, H. J. The emergence of perovskite solar cells. *Nat. Photonics* **2014**, *8*, 506−514.
(2) Stranks, S. D.; Snaith, H. J. Metal-halide perovskites for photovoltaic and light-emitting devices. *Nat. Nanotechnol.* **2015**, *10*, 391−402.
(3) Kim, M.; Jeong, J.; Lu, H.; Lee, T. K.; Eickemeyer, F. T.; Liu, Y.; Choi, I. W.; Choi, S. J.; Jo, Y.; Kim, H. B.; Mo, S. I.; Kim, Y. K.; Lee, H.; An, N. G.; Cho, S.; Tress, W. R.; Zakeeruddin, S. M.; Hagfeldt, A.; Kim, J. Y.; Gratzel, M.; Kim, D. S. Conformal quantum dot-$SnO_2$ layers as electron transporters for efficient perovskite solar cells. *Science* **2022**, *375*, 302−306.
(4) Jiang, Q.; Tong, J.; Xian, Y.; Kerner, R. A.; Dunfield, S. P.; Xiao, C.; Scheidt, R. A.; Kuciauskas, D.; Wang, X.; Hautzinger, M. P.; Tirawat, R.; Beard, M. C.; Fenning, D. P.; Berry, J. J.; Larson, B. W.; Yan, Y.; Zhu, K. Surface reaction for efficient and stable inverted perovskite solar cells. *Nature* **2022**, *611*, 278−283.
(5) Green, M. A.; Dunlop, E. D.; Hohl-Ebinger, J.; Yoshita, M.; Kopidakis, N.; Bothe, K.; Hinken, D.; Rauer, M.; Hao, X. J. Solar cell efficiency tables (Version 60). *Progress in Photovoltaics* **2022**, *30*, 687−701.
(6) Almora, O.; Baran, D.; Bazan, G. C.; Cabrera, C. I.; Erten-Ela, S.; Forberich, K.; Guo, F.; Hauch, J.; Ho-Baillie, A. W. Y.; Jacobsson, T. J.; Janssen, R. A. J.; Kirchartz, T.; Kopidakis, N.; Loi, M. A.; Lunt, R. R.; Mathew, X.; McGehee, M. D.; Min, J.; Mitzi, D. B.; Nazeeruddin, M. K.; Nelson, J.; Nogueira, A. F.; Paetzold, U. W.; Rand, B. P.; Rau, U.; Snaith, H. J.; Unger, E.; Vaillant-Roca, L.; Yang, C. C.; Yip, H. L.; Brabec, C. J. Device performance of emerging photovoltaic materials (Version 3). *Adv. Energy Mater.* **2023**, *13*, 2203313.
(7) Hörantner, M. T.; Leijtens, T.; Ziffer, M. E.; Eperon, G. E.; Christoforo, M. G.; McGehee, M. D.; Snaith, H. J. The potential of multijunction perovskite solar cells. *ACS Energy Lett.* **2017**, *2*, 2506−2513.
(8) Shockley, W.; Queisser, H. J. Detailed balance limit of efficiency of p−n junction solar cells. *J. Appl. Phys.* **1961**, *32*, 510−519.
(9) Li, Z. Q.; Zhao, Y. Z.; Wang, X.; Sun, Y. C.; Zhao, Z. G.; Li, Y. J.; Zhou, H. P.; Chen, Q. Cost analysis of perovskite tandem photovoltaics. *Joule* **2018**, *2*, 1559−1572.
(10) Leijtens, T.; Bush, K. A.; Prasanna, R.; McGehee, M. D. Opportunities and challenges for tandem solar cells using metal halide perovskite semiconductors. *Nat. Energy* **2018**, *3*, 828−838.
(11) Akkerman, Q. A.; Manna, L. What defines a halide perovskite? *ACS Energy Lett.* **2020**, *5*, 604−610.
(12) NREL. Best research-cell efficiency chart https://www.nrel.gov/pv/interactive-cell-efficiency.html (accessed 2023-03-10).
(13) Tan, H. Japan's JET Certifies Renshine Solar's 29.0% Steady-State Efficiency for All-Perovskite Tandem Solar Cell. *Taiyang News: All About Solar Power*, January 4, 2023. https://taiyangnews.info/technology/29-0-all-perovskite-tandem-solar-cell-efficiency/ (accessed 2023-03-10).
(14) Celik, I.; Philips, A. B.; Song, Z. N.; Yan, Y. F.; Ellingson, R. J.; Heben, M. J.; Apul, D. Energy payback time (EPBT) and energy return on energy invested (EROI) of perovskite tandem photovoltaic solar cells. *IEEE J. Photovolt.* **2018**, *8*, 305−309.
(15) Thiesbrummel, J.; Peña-Camargo, F.; Brinkmann, K. O.; Gutierrez-Partida, E.; Yang, F.; Warby, J.; Albrecht, S.; Neher, D.; Riedl, T.; Snaith, H. J.; Stolterfoht, M.; Lang, F. Understanding and minimizing $V_{OC}$ losses in all-perovskite tandem photovoltaics. *Adv. Energy Mater.* **2023**, *13*, 2202674.
(16) Goyal, A.; McKechnie, S.; Pashov, D.; Tumas, W.; van Schilfgaarde, M.; Stevanovic, V. Origin of pronounced nonlinear band gap behavior in lead-tin hybrid perovskite alloys. *Chem. Mater.* **2018**, *30*, 3920−3928.
(17) Schmidt, F.; Ledermann, L.; Schäffer, A.; Snaith, H. J.; Lenz, M. Rapid sequestration of perovskite solar cell-derived lead in soil. *J. Hazard. Mater.* **2022**, *436*, 128995.
(18) Schmidt, F.; Amrein, M.; Hedwig, S.; Kober-Czerny, M.; Paracchino, A.; Holappa, V.; Suhonen, R.; Schäffer, A.; Constable, E. C.; Snaith, H. J.; Lenz, M. Organic solvent free $PbI_2$ recycling from perovskite solar cells using hot water. *J. Hazard. Mater.* **2023**, *447*, 130829.
(19) *D3.2 Life cycle analysis of CHEOPS technologies and benchmarking: final assessment.* CHEOPS, May 23, 2019 https://cheops.accelopment.com/reports/ (accessed 2023-03-10).
(20) Zhao, R.; Gu, Z.; Li, P.; Zhang, Y.; Song, Y. Flexible and wearable optoelectronic devices based on perovskites. *Adv. Mater. Technol.* **2022**, *7*, 2101124.
(21) Noel, N. K.; Stranks, S. D.; Abate, A.; Wehrenfennig, C.; Guarnera, S.; Haghighirad, A.-A.; Sadhanala, A.; Eperon, G. E.; Pathak, S. K.; Johnston, M. B.; Petrozza, A.; Herz, L. M.; Snaith, H. J. Lead-free organic−inorganic tin halide perovskites for photovoltaic applications. *Energy Environ. Sci.* **2014**, *7*, 3061−3068.
(22) Hao, F.; Stoumpos, C. C.; Cao, D. H.; Chang, R. P. H.; Kanatzidis, M. G. Lead-free solid-state organic−inorganic halide perovskite solar cells. *Nat. Photonics* **2014**, *8*, 489−494.
(23) Jiang, X.; Li, H.; Zhou, Q.; Wei, Q.; Wei, M.; Jiang, L.; Wang, Z.; Peng, Z.; Wang, F.; Zang, Z.; Xu, K.; Hou, Y.; Teale, S.; Zhou, W.; Si, R.; Gao, X.; Sargent, E. H.; Ning, Z. One-step synthesis of $SnI_2$·$DMSO_x$ adducts for high-performance tin perovskite solar cells. *J. Am. Chem. Soc.* **2021**, *143*, 10970−10976.
(24) Yu, B. B.; Chen, Z.; Zhu, Y.; Wang, Y.; Han, B.; Chen, G.; Zhang, X.; Du, Z.; He, Z. Heterogeneous 2D/3D tin-halides perovskite solar cells with certified conversion efficiency breaking 14%. *Adv. Mater.* **2021**, *33*, 2102055.

(25) Zhou, J. H.; Hao, M. W.; Zhang, Y.; Ma, X.; Dong, J. C.; Lu, F. F.; Wang, J.; Wang, N.; Zhou, Y. Y. Chemo-thermal surface dedoping for high-performance tin perovskite solar cells. *Matter* **2022**, *5*, 683−693.
(26) Aktas, E.; Rajamanickam, N.; Pascual, J.; Hu, S.; Aldamasy, M. H.; Di Girolamo, D.; Li, W.; Nasti, G.; Martínez-Ferrero, E.; Wakamiya, A.; Palomares, E.; Abate, A. Challenges and strategies toward long-term stability of lead-free tin-based perovskite solar cells. *Commun. Mater.* **2022**, *3*, 104.
(27) Cao, J. P.; Yan, F. Recent progress in tin-based perovskite solar cells. *Energy Environ. Sci.* **2021**, *14*, 1286−1325.
(28) Li, B.; Chang, B. H.; Pan, L.; Li, Z. H.; Fu, L.; He, Z. B.; Yin, L. W. Tin-based defects and passivation strategies in tin-related perovskite solar cells. *ACS Energy Lett.* **2020**, *5*, 3752−3772.
(29) Tao, S.; Schmidt, I.; Brocks, G.; Jiang, J.; Tranca, I.; Meerholz, K.; Olthof, S. Absolute energy level positions in tin- and lead-based halide perovskites. *Nat. Commun.* **2019**, *10*, 2560.
(30) Savill, K. J.; Ulatowski, A. M.; Herz, L. M. Optoelectronic properties of tin-lead halide perovskites. *ACS Energy Lett.* **2021**, *6*, 2413−2426.
(31) Claudio, E. S.; Godwin, H. A.; Magyar, J. S. Fundamental coordination chemistry, environmental chemistry, and biochemistry of lead(II). *Prog. Inorg. Chem.* **2002**, *51*, 1.
(32) Abdel-Shakour, M.; Chowdhury, T. H.; Matsuishi, K.; Bedja, I.; Moritomo, Y.; Islam, A. High-efficiency tin halide perovskite solar cells: The chemistry of Tin (II) compounds and their interaction with Lewis base additives during perovskite film formation. *Sol. RRL* **2021**, *5*, 2000606.
(33) Gu, F. D.; Ye, S. Y.; Zhao, Z. R.; Rao, H. X.; Liu, Z. W.; Bian, Z. Q.; Huang, C. H. Improving performance of lead-free formamidinium tin triiodide perovskite solar cells by tin source purification. *Sol. RRL* **2018**, *2*, 1800136.
(34) Nakamura, T.; Yakumaru, S.; Truong, M. A.; Kim, K.; Liu, J.; Hu, S.; Otsuka, K.; Hashimoto, R.; Murdey, R.; Sasamori, T.; Kim, H. D.; Ohkita, H.; Handa, T.; Kanemitsu, Y.; Wakamiya, A. Sn(IV)-free tin perovskite films realized by in situ Sn(0) nanoparticle treatment of the precursor solution. *Nat. Commun.* **2020**, *11*, 3008.
(35) Morteza Najarian, A.; Vafaie, M.; Johnston, A.; Zhu, T.; Wei, M.; Saidaminov, M. I.; Hou, Y.; Hoogland, S.; García de Arquer, F. P.; Sargent, E. H. Sub-millimetre light detection and ranging using perovskites. *Nat. Electron.* **2022**, *5*, 511−518.
(36) Kumar, M. H.; Dharani, S.; Leong, W. L.; Boix, P. P.; Prabhakar, R. R.; Baikie, T.; Shi, C.; Ding, H.; Ramesh, R.; Asta, M.; Graetzel, M.; Mhaisalkar, S. G.; Mathews, N. Lead-free halide perovskite solar cells with high photocurrents realized through vacancy modulation. *Adv. Mater.* **2014**, *26*, 7122−7127.
(37) Chen, Q. Y.; Luo, J. C.; He, R.; Lai, H. G.; Ren, S. Q.; Jiang, Y. T.; Wan, Z. X.; Wang, W. W.; Hao, X.; Wang, Y.; Zhang, J. Q.; Constantinou, I.; Wang, C. L.; Wu, L. L.; Fu, F.; Zhao, D. W. Unveiling roles of tin fluoride additives in high-efficiency low-bandgap mixed tin-lead perovskite solar cells. *Adv. Energy Mater.* **2021**, *11*, 2101045.
(38) Pascual, J.; Flatken, M.; Felix, R.; Li, G.; Turren-Cruz, S. H.; Aldamasy, M. H.; Hartmann, C.; Li, M.; Di Girolamo, D.; Nasti, G.; Husam, E.; Wilks, R. G.; Dallmann, A.; Bar, M.; Hoell, A.; Abate, A. Fluoride chemistry in tin halide perovskites. *Angew. Chem., Int. Ed.* **2021**, *60*, 21583−21591.
(39) Kurisinkal Pious, J.; Zwirner, Y.; Lai, H.; Olthof, S.; Jeangros, Q.; Gilshtein, E.; Kothandaraman, R. K.; Artuk, K.; Wechsler, P.; Chen, C.; Wolff, C. M.; Zhao, D.; Tiwari, A. N.; Fu, F. Revealing the role of tin fluoride additive in narrow bandgap Pb-Sn perovskites for highly efficient flexible all-perovskite tandem cells. *ACS Appl. Mater. Interfaces* **2023**, *15*, 10150−10157.
(40) Savill, K. J.; Ulatowski, A. M.; Farrar, M. D.; Johnston, M. B.; Snaith, H. J.; Herz, L. M. Impact of tin fluoride additive on the properties of mixed tin-lead iodide perovskite semiconductors. *Adv. Funct. Mater.* **2020**, *30*, 2005594.
(41) Hu, S.; Truong, M. A.; Otsuka, K.; Handa, T.; Yamada, T.; Nishikubo, R.; Iwasaki, Y.; Saeki, A.; Murdey, R.; Kanemitsu, Y.; Wakamiya, A. Mixed lead-tin perovskite films with > 7 $\mu$s charge carrier lifetimes realized by maltol post-treatment. *Chem. Sci.* **2021**, *12*, 13513−13519.
(42) Meggiolaro, D.; Ricciarelli, D.; Alasmari, A. A.; Alasmary, F. A. S.; De Angelis, F. Tin versus lead redox chemistry modulates charge trapping and self-doping in tin/lead iodide perovskites. *J. Phys. Chem. Lett.* **2020**, *11*, 3546−3556.
(43) Mundt, L. E.; Tong, J. H.; Palmstrom, A. F.; Dunfield, S. P.; Zhu, K.; Berry, J. J.; Schelhas, L. T.; Ratcliff, E. L. Surface-activated corrosion in tin-lead halide perovskite solar cells. *ACS Energy Lett.* **2020**, *5*, 3344−3351.
(44) Ricciarelli, D.; Meggiolaro, D.; Ambrosio, F.; De Angelis, F. Instability of tin iodide perovskites: Bulk p-doping versus surface tin oxidation. *ACS Energy Lett.* **2020**, *5*, 2787−2795.
(45) Mitzi, D. B.; Feild, C. A.; Harrison, W. T. A.; Guloy, A. M. Conducting tin halides with a layered organic-based perovskite structure. *Nature* **1994**, *369*, 467−469.
(46) Li, X.; Hoffman, J.; Ke, W.; Chen, M.; Tsai, H.; Nie, W.; Mohite, A. D.; Kepenekian, M.; Katan, C.; Even, J.; Wasielewski, M. R.; Stoumpos, C. C.; Kanatzidis, M. G. Two-dimensional halide perovskites incorporating straight chain symmetric diammonium ions, $(NH_3C_mH_{2m}NH_3)(CH_3NH_3)_{n-1}PbnI_{3n+1}$ (m = 4−9; n = 1−4). *J. Am. Chem. Soc.* **2018**, *140*, 12226−12238.
(47) Li, X.; Hoffman, J. M.; Kanatzidis, M. G. The 2D halide perovskite rulebook: How the spacer influences everything from the structure to optoelectronic device efficiency. *Chem. Rev.* **2021**, *121*, 2230−2291.
(48) Tong, J.; Song, Z.; Kim, D. H.; Chen, X.; Chen, C.; Palmstrom, A. F.; Ndione, P. F.; Reese, M. O.; Dunfield, S. P.; Reid, O. G.; Liu, J.; Zhang, F.; Harvey, S. P.; Li, Z.; Christensen, S. T.; Teeter, G.; Zhao, D.; Al-Jassim, M. M.; van Hest, M. F. A. M.; Beard, M. C.; Shaheen, S. E.; Berry, J. J.; Yan, Y.; Zhu, K. Carrier lifetimes of > 1 $\mu$s in Sn−Pb perovskites enable efficient all-perovskite tandem solar cells. *Science* **2019**, *364*, 475.
(49) Tong, J. H.; Jiang, Q.; Ferguson, A. J.; Palmstrom, A. F.; Wang, X. M.; Hao, J.; Dunfield, S. P.; Louks, A. E.; Harvey, S. P.; Li, C. W.; Lu, H. P.; France, R. M.; Johnson, S. A.; Zhang, F.; Yang, M. J.; Geisz, J. F.; McGehee, M. D.; Beard, M. C.; Yan, Y. F.; Kuciauskas, D.; Berry, J. J.; Zhu, K. Carrier control in Sn−Pb perovskites via 2D cation engineering for all-perovskite tandem solar cells with improved efficiency and stability. *Nat. Energy* **2022**, *7*, 642−651.
(50) Gao, Y.; Wei, Z.; Yoo, P.; Shi, E.; Zeller, M.; Zhu, C.; Liao, P.; Dou, L. Highly stable lead-free perovskite field-effect transistors incorporating linear $\pi$-conjugated organic ligands. *J. Am. Chem. Soc.* **2019**, *141*, 15577−15585.
(51) Jiang, X.; Wang, F.; Wei, Q.; Li, H.; Shang, Y.; Zhou, W.; Wang, C.; Cheng, P.; Chen, Q.; Chen, L.; Ning, Z. Ultra-high open-circuit voltage of tin perovskite solar cells via an electron transporting layer design. *Nat. Commun.* **2020**, *11*, 1245.
(52) Leijtens, T.; Prasanna, R.; Gold-Parker, A.; Toney, M. F.; McGehee, M. D. Mechanism of tin oxidation and stabilization by lead substitution in tin halide perovskites. *ACS Energy Lett.* **2017**, *2*, 2159−2165.
(53) Lim, V. J. Y.; Ulatowski, A. M.; Kamaraki, C.; Klug, M. T.; Perez, L. M.; Johnston, M. B.; Herz, L. M. Air-degradation mechanisms in mixed lead-tin halide perovskites for solar cells. *Adv. Energy Mater.* **2022**, 2200847.
(54) Ambrosio, F.; Meggiolaro, D.; Almutairi, T. M.; De Angelis, F. Composition-dependent struggle between iodine and tin chemistry at the surface of mixed tin/lead perovskites. *ACS Energy Lett.* **2021**, *6*, 969−976.
(55) Park, C.; Choi, J.; Min, J.; Cho, K. Suppression of oxidative degradation of tin-lead hybrid organometal halide perovskite solar cells by Ag doping. *ACS Energy Lett.* **2020**, *5*, 3285−3294.
(56) Sahamir, S. R.; Kamarudin, M. A.; Ripolles, T. S.; Baranwal, A. K.; Kapil, G.; Shen, Q.; Segawa, H.; Bisquert, J.; Hayase, S. Enhancing the electronic properties and stability of high-efficiency tin-lead mixed halide perovskite solar cells via doping engineering. *J. Phys. Chem. Lett.* **2022**, *13*, 3130−3137.


https://doi.org/10.1021/prechem.3c00018
*Precis. Chem.* 2023, 1, 69−82

(57) Yu, Z.; Chen, X.; Harvey, S. P.; Ni, Z.; Chen, B.; Chen, S.; Yao, C.; Xiao, X.; Xu, S.; Yang, G.; Yan, Y.; Berry, J. J.; Beard, M. C.; Huang, J. Gradient doping in Sn-Pb perovskites by barium ions for efficient single-junction and tandem solar cells. *Adv. Mater.* **2022**, *34*, 2110351.
(58) Adjokatse, S.; Kahmann, S.; Duim, H.; Loi, M. A. Effects of strontium doping on the morphological, structural, and photophysical properties of $FASnI_3$ perovskite thin films. *APL Mater.* **2019**, *7*, 031116.
(59) Bowman, A. R.; Klug, M. T.; Doherty, T. A. S.; Farrar, M. D.; Senanayak, S. P.; Wenger, B.; Divitini, G.; Booker, E. P.; Andaji-Garmaroudi, Z.; Macpherson, S.; Ruggeri, E.; Sirringhaus, H.; Snaith, H. J.; Stranks, S. D. Microsecond carrier lifetimes, controlled p-doping, and enhanced air stability in low-bandgap metal halide perovskites. *ACS Energy Lett.* **2019**, *4*, 2301−2307.
(60) Bian, H.; You, J.; Xu, C.; He, X.; Wang, M.; Yao, Y.; Zeng, W.; Guo, P.; Zhou, H.; Lu, D.; Dai, Z.; Zhang, S.; Song, Q. Chemically suppressing redox reaction at the NiOx/perovskite interface in narrow bandgap perovskite solar cells to exceed a power conversion efficiency of 20%. *J. Mater. Chem. A* **2022**, *11*, 205−212.
(61) Chen, M.; Dong, Q.; Xiao, C.; Zheng, X.; Dai, Z.; Shi, Y.; Luther, J. M.; Padture, N. P. Lead-free flexible perovskite solar cells with interfacial native oxide have > 10% efficiency and simultaneously enhanced stability and reliability. *ACS Energy Lett.* **2022**, *7*, 2256−2264.
(62) Chen, B.; Yu, Z.; Onno, A.; Yu, Z.; Chen, S.; Wang, J.; Holman, Z. C.; Huang, J. Bifacial all-perovskite tandem solar cells. *Sci. Adv.* **2022**, *8*, eadd0377.
(63) Pascual, J.; Nasti, G.; Aldamasy, M. H.; Smith, J. A.; Flatken, M.; Phung, N.; Di Girolamo, D.; Turren-Cruz, S. H.; Li, M.; Dallmann, A.; Avolio, R.; Abate, A. Origin of Sn(II) oxidation in tin halide perovskites. *Mater. Adv.* **2020**, *1*, 1066−1070.
(64) Saidaminov, M. I.; Spanopoulos, I.; Abed, J.; Ke, W. J.; Wicks, J.; Kanatzidis, M. G.; Sargent, E. H. Conventional solvent oxidizes Sn(II) in perovskite inks. *ACS Energy Lett.* **2020**, *5*, 1153−1155.
(65) Mahmud, M. A.; Zheng, J. H.; Tang, S.; Liao, W. H.; Wang, G. L.; Bing, J. M.; Leung, T. L.; Bui, A. D.; Chen, H. J.; Yi, J. P.; Bremner, S. P.; Nguyen, H. T.; Ho-Baillie, A. W. Y. Water-free, conductive hole transport layer for reproducible perovskite-perovskite tandems with record fill factor. *ACS Energy Lett.* **2023**, *8*, 21−30.
(66) Wang, J. T.; Yu, Z. H.; Astridge, D. D.; Ni, Z. Y.; Zhao, L.; Chen, B.; Wang, M. R.; Zhou, Y.; Yang, G.; Dai, X. Z.; Sellinger, A.; Huang, J. S. Carbazole-based hole transport polymer for methylammonium-free tin-lead perovskite solar cells with enhanced efficiency and stability. *ACS Energy Lett.* **2022**, *7*, 3353−3361.
(67) Yu, Z.; Wang, J.; Chen, B.; Uddin, M. A.; Ni, Z.; Yang, G.; Huang, J. Solution-processed ternary tin(II) alloy as hole-transport layer of Sn−Pb perovskite solar cells for enhanced efficiency and stability. *Adv. Mater.* **2022**, *34*, 2205769.
(68) Park, K.; Lee, J. H.; Lee, J. W. Surface defect engineering of metal halide perovskites for photovoltaic applications. *ACS Energy Lett.* **2022**, *7*, 1230−1239.
(69) Di Girolamo, D.; Pascual, J.; Aldamasy, M. H.; Iqbal, Z.; Li, G.; Radicchi, E.; Li, M.; Turren-Cruz, S.-H.; Nasti, G.; Dallmann, A.; De Angelis, F.; Abate, A. Solvents for processing stable tin halide perovskites. *ACS Energy Lett.* **2021**, *6*, 959−968.
(70) Ball, J. M.; Buizza, L.; Sansom, H. C.; Farrar, M. D.; Klug, M. T.; Borchert, J.; Patel, J.; Herz, L. M.; Johnston, M. B.; Snaith, H. J. Dual-source coevaporation of low-bandgap $FA_{1-x}Cs_xSn_{1-y}Pb_yI_3$ perovskites for photovoltaics. *ACS Energy Lett.* **2019**, *4*, 2748−2756.
(71) Igual-Muñoz, A. M.; Castillo, A.; Dreessen, C.; Boix, P. P.; Bolink, H. J. Vacuum-deposited multication tin−lead perovskite solar cells. *ACS Appl. Energy Mater.* **2020**, *3*, 2755−2761.
(72) Ma, S.; Yuan, G.; Zhang, Y.; Yang, N.; Li, Y.; Chen, Q. Development of encapsulation strategies towards the commercialization of perovskite solar cells. *Energy Environ. Sci.* **2022**, *15*, 13−55.
(73) Liang, K. N.; Mitzi, D. B.; Prikas, M. T. Synthesis and characterization of organic-inorganic perovskite thin films prepared using a versatile two-step dipping technique. *Chem. Mater.* **1998**, *10*, 403−411.
(74) Hao, F.; Stoumpos, C. C.; Chang, R. P.; Kanatzidis, M. G. Anomalous band gap behavior in mixed Sn and Pb perovskites enables broadening of absorption spectrum in solar cells. *J. Am. Chem. Soc.* **2014**, *136*, 8094−8099.
(75) Zhu, H. L.; Lin, H.; Song, Z.; Wang, Z.; Ye, F.; Zhang, H.; Yin, W. J.; Yan, Y.; Choy, W. C. H. Achieving high-quality Sn-Pb perovskite films on complementary metal-oxide-semiconductor-compatible metal/silicon substrates for efficient imaging array. *ACS Nano* **2019**, *13*, 11800−11808.
(76) Dong, J. J.; Shao, S. Y.; Kahmann, S.; Rommens, A. J.; Hermida-Merino, D.; ten Brink, G. H.; Loi, M. A.; Portale, G. Mechanism of crystal formation in Ruddlesden-Popper Sn-based perovskites. *Adv. Funct. Mater.* **2020**, *30*, 2001294.
(77) Dong, H.; Ran, C.; Gao, W.; Sun, N.; Liu, X.; Xia, Y.; Chen, Y.; Huang, W. Crystallization dynamics of Sn-based perovskite thin films: Toward efficient and stable photovoltaic devices. *Adv. Energy Mater.* **2022**, *12*, 2102213.
(78) Liu, H.; Zhang, Z.; Zuo, W.; Roy, R.; Li, M.; Byranvand, M. M.; Saliba, M. Pure tin halide perovskite solar cells: Focusing on preparation and strategies. *Adv. Energy Mater.* **2023**, *13*, 2202209.
(79) Su, Y.; Yang, J.; Liu, G.; Sheng, W.; Zhang, J.; Zhong, Y.; Tan, L.; Chen, Y. Acetic acid-assisted synergistic modulation of crystallization kinetics and inhibition of $Sn^{2+}$ oxidation in tin-based perovskite solar cells. *Adv. Funct. Mater.* **2022**, *32*, 2109631.
(80) Wang, S. R.; Zhang, X.; Zhu, W. K.; Tang, Z. Y.; Liu, J. K.; Zhang, H.; Ding, L. M.; Hao, F. Lewis base manipulated crystallization for efficient tin halide perovskite solar cells. *Appl. Surf. Sci.* **2022**, *602*, 154393.
(81) Hu, S.; Otsuka, K.; Murdey, R.; Nakamura, T.; Truong, M. A.; Yamada, T.; Handa, T.; Matsuda, K.; Nakano, K.; Sato, A.; Marumoto, K.; Tajima, K.; Kanemitsu, Y.; Wakamiya, A. Optimized carrier extraction at interfaces for 23.6% efficient tin−lead perovskite solar cells. *Energy Environ. Sci.* **2022**, *15*, 2096−2107.
(82) Wang, M.; Wang, W.; Shen, Y.; Ma, J.; Shen, W.; Cao, K.; Liu, L.; Chen, S. Stirring-time control approach to manage colloid nucleation size for the fabrication of high-performance Sn-based perovskite solar cells. *ACS Appl. Mater. Interfaces* **2022**, *14*, 53960−53970.
(83) Meng, X.; Li, Y.; Qu, Y.; Chen, H.; Jiang, N.; Li, M.; Xue, D. J.; Hu, J. S.; Huang, H.; Yang, S. Crystallization kinetics modulation of $FASnI_3$ films with pre-nucleation clusters for efficient lead-free perovskite solar cells. *Angew. Chem., Int. Ed.* **2021**, *60*, 3693−3698.
(84) Noel, N. K.; Congiu, M.; Ramadan, A. J.; Fearn, S.; McMeekin, D. P.; Patel, J. B.; Johnston, M. B.; Wenger, B.; Snaith, H. J. Unveiling the influence of pH on the crystallization of hybrid perovskites, delivering low voltage loss photovoltaics. *Joule* **2017**, *1*, 328−343.
(85) Zhang, Z.; Liang, J.; Wang, J.; Zheng, Y.; Wu, X.; Tian, C.; Sun, A.; Chen, Z.; Chen, C. C. Resolving mixed intermediate phases in methylammonium-free Sn-Pb alloyed perovskites for high-performance solar cells. *Nano-Micro Lett.* **2022**, *14*, 165.
(86) O'Kane, M. E.; Smith, J. A.; Kilbride, R. C.; Spooner, E. L. K.; Duif, C. P.; Catley, T. E.; Washington, A. L.; King, S. M.; Parnell, S. R.; Parnell, A. J. Exploring nanoscale structure in perovskite precursor solutions using neutron and light scattering. *Chem. Mater.* **2022**, *34*, 7232−7241.
(87) Dutta, N. S.; Noel, N. K.; Arnold, C. B. Crystalline nature of colloids in methylammonium lead halide perovskite precursor inks revealed by cryo-electron microscopy. *J. Phys. Chem. Lett.* **2020**, *11*, 5980−5986.
(88) Shargaieva, O.; Nasstrom, H.; Smith, J. A.; Tobbens, D.; Munir, R.; Unger, E. Hybrid perovskite crystallization from binary solvent mixtures: Interplay of evaporation rate and binding strength of solvents. *Mater. Adv.* **2020**, *1*, 3314−3321.
(89) Radicchi, E.; Mosconi, E.; Elisei, F.; Nunzi, F.; De Angelis, F. Understanding the solution chemistry of lead halide perovskites precursors. *ACS Appl. Energy Mater.* **2019**, *2*, 3400−3409.
(90) Kaiser, W.; Radicchi, E.; Mosconi, E.; Kachmar, A.; De Angelis, F. Iodide vs chloride: The impact of different lead halides on the solution chemistry of perovskite precursors. *ACS Appl. Energy Mater.* **2021**, *4*, 9827−9835.
(91) Cao, X. R.; Li, J. R.; Dong, H.; Li, P. Z.; Fan, Q. H.; Xu, R. Y.; Li, H. M.; Zhou, G. J.; Wu, Z. X. Stability improvement of tin-based halide

perovskite by precursor-solution regulation with dual-functional reagents. *Adv. Funct. Mater.* **2021**, *31*, 2104344.
(92) He, L. T.; Gu, H.; Liu, X. L.; Li, P. W.; Dang, Y. Y.; Liang, C.; Ono, L. K.; Qi, Y. B.; Tao, X. T. Efficient anti-solvent-free spin-coated and printed Sn-perovskite solar cells with crystal-based precursor solutions. *Matter* **2020**, *2*, 167−180.
(93) Ozaki, M.; Katsuki, Y.; Liu, J.; Handa, T.; Nishikubo, R.; Yakumaru, S.; Hashikawa, Y.; Murata, Y.; Saito, T.; Shimakawa, Y.; Kanemitsu, Y.; Saeki, A.; Wakamiya, A. Solvent-coordinated tin halide complexes as purified precursors for tin-based perovskites. *ACS Omega* **2017**, *2*, 7016−7021.
(94) Hao, F.; Stoumpos, C. C.; Guo, P.; Zhou, N.; Marks, T. J.; Chang, R. P.; Kanatzidis, M. G. Solvent-mediated crystallization of $CH_3NH_3SnI_3$ films for heterojunction depleted perovskite solar cells. *J. Am. Chem. Soc.* **2015**, *137*, 11445−11452.
(95) Cao, J.; Jing, X.; Yan, J.; Hu, C.; Chen, R.; Yin, J.; Li, J.; Zheng, N. Identifying the molecular structures of intermediates for optimizing the fabrication of high-quality perovskite films. *J. Am. Chem. Soc.* **2016**, *138*, 9919−9926.
(96) Cheng, F. W.; Jing, X. J.; Chen, R. H.; Cao, J.; Yan, J. Z.; Wu, Y. Y. Q.; Huang, X. F.; Wu, B. H.; Zheng, N. F. N-Methyl-2-pyrrolidone as an excellent coordinative additive with a wide operating range for fabricating high-quality perovskite films. *Inorg. Chem. Front.* **2019**, *6*, 2458−2463.
(97) Smith, P. J. *Chemistry of tin*; Springer: Dordrecht, 2012; https://link.springer.com/book/10.1007/978-94-011-4938-9.
(98) Walsh, A.; Watson, G. W. Influence of the anion on lone pair formation in Sn(II) monochalcogenides: A DFT study. *J. Phys. Chem. B* **2005**, *109*, 18868−18875.
(99) Persson, I.; D'Angelo, P.; Lundberg, D. Hydrated and solvated tin(II) ions in solution and the solid state, and a coordination chemistry overview of the $d^{10}s^2$ metal ions. *Chem.-Eur. J.* **2016**, *22*, 18583−18592.
(100) Gratia, P.; Zimmermann, I.; Schouwink, P.; Yum, J. H.; Audinot, J. N.; Sivula, K.; Wirtz, T.; Nazeeruddin, M. K. The many faces of mixed ion perovskites: Unraveling and understanding the crystallization process. *ACS Energy Lett.* **2017**, *2*, 2686−2693.
(101) Stoumpos, C. C.; Mao, L.; Malliakas, C. D.; Kanatzidis, M. G. Structure-band gap relationships in hexagonal polytypes and low-dimensional structures of hybrid tin iodide perovskites. *Inorg. Chem.* **2017**, *56*, 56−73.
(102) Pitaro, M.; Tekelenburg, E. K.; Shao, S.; Loi, M. A. Tin halide perovskites: From fundamental properties to solar cells. *Adv. Mater.* **2022**, *34*, 2105844.
(103) Wang, J. K.; Datta, K.; Li, J. Y.; Verheijen, M. A.; Zhang, D.; Wienk, M. M.; Janssen, R. A. J. Understanding the film formation kinetics of sequential deposited narrow-bandgap Pb-Sn hybrid perovskite films. *Adv. Energy Mater.* **2020**, *10*, 2000566.
(104) Bandara, R. M. I.; Jayawardena, K. D. G. I.; Adeyemo, S. O.; Hinder, S. J.; Smith, J. A.; Thirimanne, H. M.; Wong, N. C.; Amin, F. M.; Freestone, B. G.; Parnell, A. J.; Lidzey, D. G.; Joyce, H. J.; Sporea, R. A.; Silva, S. R. P. Tin(IV) dopant removal through anti-solvent engineering enabling tin based perovskite solar cells with high charge carrier mobilities. *J. Mater. Chem. C* **2019**, *7*, 8389−8397.
(105) Werner, J.; Moot, T.; Gossett, T. A.; Gould, I. E.; Palmstrom, A. F.; Wolf, E. J.; Boyd, C. C.; van Hest, M. F. A. M.; Luther, J. M.; Berry, J. J.; McGehee, M. D. Improving low-bandgap tin-lead perovskite solar cells via contact engineering and gas quench processing. *ACS Energy Lett.* **2020**, *5*, 1215−1223.
(106) Liu, X.; Wu, T.; Luo, X.; Wang, H.; Furue, M.; Bessho, T.; Zhang, Y.; Nakazaki, J.; Segawa, H.; Han, L. Lead-free perovskite solar cells with over 10% efficiency and size 1 $cm^2$ enabled by solvent−crystallization regulation in a two-step deposition method. *ACS Energy Lett.* **2022**, *7*, 425−431.
(107) Lv, S. S.; Gao, W. Y.; Ran, C. X.; Li, D. L.; Chao, L. F.; Wang, X. B.; Song, L.; Lin, Z. Q.; Fu, L.; Chen, Y. H. Antisolvent-free fabrication of efficient and stable Sn-Pb perovskite solar cells. *Sol. RRL* **2021**, *5*, 2100675.
(108) Dong, H.; Ran, C. X.; Li, W. Y.; Liu, X.; Gao, W. Y.; Xia, Y. D.; Chen, Y. H.; Huang, W. Reductive ionic liquid-mediated crystallization for enhanced photovoltaic performance of Sn-based perovskite solar cells. *Sci. China Chem.* **2022**, *65*, 1895−1902.
(109) Klug, M. T.; Milot, R. L.; Patel, J. B.; Green, T.; Sansom, H. C.; Farrar, M. D.; Ramadan, A. J.; Martani, S.; Wang, Z. P.; Wenger, B.; Ball, J. M.; Langshaw, L.; Petrozza, A.; Johnston, M. B.; Herz, L. M.; Snaith, H. J. Metal composition influences optoelectronic quality in mixed-metal lead-tin triiodide perovskite solar absorbers. *Energy Environ. Sci.* **2020**, *13*, 1776−1787.
(110) Li, Z.; Li, X.; Wang, M.; Cai, M.; Shi, X.; Mo, Y.; Chen, X.; Ren, D.; Yang, M.; Liu, X.; Jia, R.; Medhekar, N. V.; Dai, S. Enhanced photovoltaic performance via a bifunctional additive in tin-based perovskite solar cells. *ACS Appl. Energy Mater.* **2022**, *5*, 108−115.
(111) Zhou, X.; Zhang, L.; Wang, X.; Liu, C.; Chen, S.; Zhang, M.; Li, X.; Yi, W.; Xu, B. Highly efficient and stable GABr-modified ideal-bandgap (1.35 eV) Sn/Pb perovskite solar cells achieve 20.63% efficiency with a record small $V_{OC}$ deficit of 0.33 V. *Adv. Mater.* **2020**, *32*, 1908107.
(112) Nishimura, K.; Kamarudin, M. A.; Hirotani, D.; Hamada, K.; Shen, Q.; Iikubo, S.; Minemoto, T.; Yoshino, K.; Hayase, S. Lead-free tin-halide perovskite solar cells with 13% efficiency. *Nano Energy* **2020**, *74*, 104858.
(113) Juarez-Perez, E. J.; Hawash, Z.; Raga, S. R.; Ono, L. K.; Qi, Y. B. Thermal degradation of $CH_3NH_3PbI_3$ perovskite into $NH_3$ and $CH_3I$ gases observed by coupled thermogravimetry-mass spectrometry analysis. *Energy Environ. Sci.* **2016**, *9*, 3406−3410.
(114) Perini, C. A. R.; Rojas-Gatjens, E.; Ravello, M.; Castro-Mendez, A. F.; Hidalgo, J.; An, Y.; Kim, S.; Lai, B.; Li, R.; Silva-Acuna, C.; Correa-Baena, J. P. Interface reconstruction from ruddlesden-popper structures impacts stability in lead halide perovskite solar cells. *Adv. Mater.* **2022**, *34*, 2270350.
(115) Kim, M.; Kim, G. H.; Lee, T. K.; Choi, I. W.; Choi, H. W.; Jo, Y.; Yoon, Y. J.; Kim, J. W.; Lee, J.; Huh, D.; Lee, H.; Kwak, S. K.; Kim, J. Y.; Kim, D. S. Methylammonium chloride induces intermediate phase stabilization for efficient perovskite solar cells. *Joule* **2019**, *3*, 2179−2192.
(116) Parikh, N.; Pandey, M.; Prochowicz, D.; Kalam, A.; Tavakoli, M. M.; Satapathi, S.; Akin, S.; Yadav, P. Investigation on the facet-dependent anisotropy in halide perovskite single crystals. *J. Phys. Chem. C* **2022**, *126*, 8906−8912.
(117) Ball, J. M.; Petrozza, A. Defects in perovskite-halides and their effects in solar cells. *Nat. Energy* **2016**, *1*, 16149.
(118) Brandt, R. E.; Poindexter, J. R.; Gorai, P.; Kurchin, R. C.; Hoye, R. L. Z.; Nienhaus, L.; Wilson, M. W. B.; Polizzotti, J. A.; Sereika, R.; Zaltauskas, R.; Lee, L. C.; MacManus-Driscoll, J. L.; Bawendi, M.; Stevanovic, V.; Buonassisi, T. Searching for "defect-tolerant" photovoltaic materials: Combined theoretical and experimental screening. *Chem. Mater.* **2017**, *29*, 4667−4674.
(119) Xu, J.; Maxwell, A.; Wei, M. Y.; Wang, Z. W.; Chen, B.; Zhu, T.; Sargent, E. H. Defect tolerance of mixed B-site organic-inorganic halide perovskites. *ACS Energy Lett.* **2021**, *6*, 4220−4227.
(120) Luo, D. Y.; Su, R.; Zhang, W.; Gong, Q. H.; Zhu, R. Minimizing non-radiative recombination losses in perovskite solar cells. *Nat. Rev. Mater.* **2020**, *5*, 44−60.
(121) Xu, P.; Chen, S.; Xiang, H.-J.; Gong, X.-G.; Wei, S.-H. Influence of defects and synthesis conditions on the photovoltaic performance of perovskite semiconductor $CsSnI_3$. *Chem. Mater.* **2014**, *26*, 6068−6072.
(122) Shi, T. T.; Zhang, H. S.; Meng, W. W.; Teng, Q.; Liu, M. Y.; Yang, X. B.; Yan, Y. F.; Yip, H. L.; Zhao, Y. J. Effects of organic cations on the defect physics of tin halide perovskites. *J. Mater. Chem. A* **2017**, *5*, 15124−15129.
(123) Liu, Q.; Li, A.; Chu, W.; Prezhdo, O. V.; Liang, W. Influence of intrinsic defects on the structure and dynamics of the mixed Pb−Sn perovskite: First-principles DFT and NAMD simulations. *J. Mater. Chem. A* **2021**, *10*, 234−244.
(124) Lanzetta, L.; Webb, T.; Zibouche, N.; Liang, X.; Ding, D.; Min, G.; Westbrook, R. J. E.; Gaggio, B.; Macdonald, T. J.; Islam, M. S.; Haque, S. A. Degradation mechanism of hybrid tin-based perovskite solar cells and the critical role of tin(IV) iodide. *Nat. Commun.* **2021**, *12*, 2853.

(125) Jiang, X. Y.; Zang, Z. H.; Zhou, Y. Y.; Li, H. S.; Wei, Q.; Ning, Z. J. Tin halide perovskite solar cells: An emerging thin-film photovoltaic technology. *Acc. Mater. Res.* **2021**, *2*, 210−219.
(126) Zhang, Z.; Qiao, L.; Meng, K.; Long, R.; Chen, G.; Gao, P. Rationalization of passivation strategies toward high-performance perovskite solar cells. *Chem. Soc. Rev.* **2023**, *52*, 163−195.
(127) Hu, S.; Zhao, P.; Nakano, K.; Oliver, R. D. J.; Pascual, J.; Smith, J. A.; Yamada, T.; Truong, M. A.; Murdey, R.; Shioya, N.; Hasegawa, T.; Ehara, M.; Johnston, M. B.; Tajima, K.; Kanemitsu, Y.; Snaith, H. J.; Wakamiya, A. Synergistic surface modification of tin-lead perovskite solar cells. *Adv. Mater.* **2023**, *35*, 2208320.
(128) Li, W. H.; Yadavalli, S. K.; Lizarazo-Ferro, D.; Chen, M.; Zhou, Y. Y.; Padture, N. P.; Zia, R. Subgrain special boundaries in halide perovskite thin films restrict carrier diffusion. *ACS Energy Lett.* **2018**, *3*, 2669−2670.
(129) Jariwala, S.; Sun, H. Y.; Adhyaksa, G. W. P.; Lof, A.; Muscarella, L. A.; Ehrler, B.; Garnett, E. C.; Ginger, D. S. Local crystal misorientation influences non-radiative recombination in halide perovskites. *Joule* **2019**, *3*, 3048−3060.
(130) Doherty, T. A. S.; Winchester, A. J.; Macpherson, S.; Johnstone, D. N.; Pareek, V.; Tennyson, E. M.; Kosar, S.; Kosasih, F. U.; Anaya, M.; Abdi-Jalebi, M.; Andaji-Garmaroudi, Z.; Wong, E. L.; Madeo, J.; Chiang, Y. H.; Park, J. S.; Jung, Y. K.; Petoukhoff, C. E.; Divitini, G.; Man, M. K. L.; Ducati, C.; Walsh, A.; Midgley, P. A.; Dani, K. M.; Stranks, S. D. Performance-limiting nanoscale trap clusters at grain junctions in halide perovskites. *Nature* **2020**, *580*, 360−366.
(131) Savill, K. J.; Ulatowski, A. M.; Herz, L. M. Optoelectronic properties of tin-lead halide perovskites. *ACS Energy Lett.* **2021**, *6*, 2413−2426.
(132) Senanayak, S. P.; Dey, K.; Shivanna, R.; Li, W.; Ghosh, D.; Zhang, Y.; Roose, B.; Zelewski, S. J.; Andaji-Garmaroudi, Z.; Wood, W.; Tiwale, N.; MacManus-Driscoll, J. L.; Friend, R. H.; Stranks, S. D.; Sirringhaus, H. Charge transport in mixed metal halide perovskite semiconductors. *Nat. Mater.* **2023**, *22*, 216−224.
(133) Thiesbrummel, J.; Le Corre, V. M.; Peña-Camargo, F.; Perdigón-Toro, L.; Lang, F.; Yang, F.; Grischek, M.; Gutierrez-Partida, E.; Warby, J.; Farrar, M. D.; Mahesh, S.; Caprioglio, P.; Albrecht, S.; Neher, D.; Snaith, H. J.; Stolterfoht, M. Universal current losses in perovskite solar cells due to mobile ions. *Adv. Energy Mater.* **2021**, *11*, 2101447.
(134) Moia, D.; Gelmetti, I.; Calado, P.; Fisher, W.; Stringer, M.; Game, O.; Hu, Y.; Docampo, P.; Lidzey, D.; Palomares, E.; Nelson, J.; Barnes, P. R. F. Ionic-to-electronic current amplification in hybrid perovskite solar cells: ionically gated transistor-interface circuit model explains hysteresis and impedance of mixed conducting devices. *Energy Environ. Sci.* **2019**, *12*, 1296−1308.
(135) Boehm, A. M.; Liu, T.; Park, S. M.; Abtahi, A.; Graham, K. R. Influence of surface ligands on energetics at $FASnI_3/C_{60}$ interfaces and their impact on photovoltaic performance. *ACS Appl. Mater. Interfaces* **2020**, *12*, 5209−5218.
(136) Ighodalo, K. O.; Chen, W.; Liang, Z.; Shi, Y.; Chu, S.; Zhang, Y.; Khan, R.; Zhou, H.; Pan, X.; Ye, J.; Xiao, Z. Negligible ion migration in tin-based and tin-doped perovskites. *Angew. Chem., Int. Ed.* **2023**, *62*, 202213932.
(137) Ke, W.; Priyanka, P.; Vegiraju, S.; Stoumpos, C. C.; Spanopoulos, I.; Soe, C. M. M.; Marks, T. J.; Chen, M. C.; Kanatzidis, M. G. Dopant-free tetrakis-triphenylamine hole transporting material for efficient tin-based perovskite solar cells. *J. Am. Chem. Soc.* **2018**, *140*, 388−393.
(138) Hamada, K.; Tanaka, R.; Kamarudin, M. A.; Shen, Q.; Iikubo, S.; Minemoto, T.; Yoshino, K.; Toyoda, T.; Ma, T.; Kang, D. W.; Hayase, S. Enhanced device performance with passivation of the $TiO_2$ surface using a carboxylic acid fullerene monolayer for a SnPb perovskite solar cell with a normal planar structure. *ACS Appl. Mater. Interfaces* **2020**, *12*, 17776−17782.
(139) Liu, A.; Zhu, H.; Bai, S.; Reo, Y.; Zou, T.; Kim, M.-G.; Noh, Y.-Y. High-performance inorganic metal halide perovskite transistors. *Nat. Electron.* **2022**, *5*, 78−83.
(140) Kagan, C. R.; Mitzi, D. B.; Dimitrakopoulos, C. D. Organic-inorganic hybrid materials as semiconducting channels in thin-film field-effect transistors. *Science* **1999**, *286*, 945−947.
(141) Prasanna, R.; Leijtens, T.; Dunfield, S. P.; Raiford, J. A.; Wolf, E. J.; Swifter, S. A.; Werner, J.; Eperon, G. E.; de Paula, C.; Palmstrom, A. F.; Boyd, C. C.; van Hest, M. F. A. M.; Bent, S. F.; Teeter, G.; Berry, J. J.; McGehee, M. D. Design of low bandgap tin−lead halide perovskite solar cells to achieve thermal, atmospheric and operational stability. *Nat. Energy* **2019**, *4*, 939−947.
(142) Al-Ashouri, A.; Magomedov, A.; Ross, M.; Jost, M.; Talaikis, M.; Chistiakova, G.; Bertram, T.; Marquez, J. A.; Kohnen, E.; Kasparavicius, E.; Levcenco, S.; Gil-Escrig, L.; Hages, C. J.; Schlatmann, R.; Rech, B.; Malinauskas, T.; Unold, T.; Kaufmann, C. A.; Korte, L.; Niaura, G.; Getautis, V.; Albrecht, S. Conformal monolayer contacts with lossless interfaces for perovskite single junction and monolithic tandem solar cells. *Energy Environ. Sci.* **2019**, *12*, 3356−3369.
(143) Levine, I.; Al-Ashouri, A.; Musiienko, A.; Hempel, H.; Magomedov, A.; Drevilkauskaite, A.; Getautis, V.; Menzel, D.; Hinrichs, K.; Unold, T.; Albrecht, S.; Dittrich, T. Charge transfer rates and electron trapping at buried interfaces of perovskite solar cells. *Joule* **2021**, *5*, 2915−2933.
(144) Song, D.; Narra, S.; Li, M. Y.; Lin, J. S.; Diau, E. W. G. Interfacial engineering with a hole-selective self-assembled monolayer for tin perovskite solar cells via a two-step fabrication. *ACS Energy Lett.* **2021**, *6*, 4179−4186.
(145) Kapil, G.; Bessho, T.; Sanehira, Y.; Sahamir, S. R.; Chen, M. M.; Baranwal, A. K.; Liu, D.; Sono, Y. Y.; Hirotani, D.; Nomura, D.; Nishimura, K.; Kamarudin, M. A.; Shen, Q.; Segawa, H.; Hayase, S. Tin-lead perovskite solar cells fabricated on hole selective monolayers. *ACS Energy Lett.* **2022**, *7*, 966−974.
(146) Al-Ashouri, A.; Kohnen, E.; Li, B.; Magomedov, A.; Hempel, H.; Caprioglio, P.; Marquez, J. A.; Morales Vilches, A. B.; Kasparavicius, E.; Smith, J. A.; Phung, N.; Menzel, D.; Grischek, M.; Kegelmann, L.; Skroblin, D.; Gollwitzer, C.; Malinauskas, T.; Jost, M.; Matic, G.; Rech, B.; Schlatmann, R.; Topic, M.; Korte, L.; Abate, A.; Stannowski, B.; Neher, D.; Stolterfoht, M.; Unold, T.; Getautis, V.; Albrecht, S. Monolithic perovskite/silicon tandem solar cell with > 29% efficiency by enhanced hole extraction. *Science* **2020**, *370*, 1300−1309.
(147) Liu, J.; Ozaki, M.; Yakumaru, S.; Handa, T.; Nishikubo, R.; Kanemitsu, Y.; Saeki, A.; Murata, Y.; Murdey, R.; Wakamiya, A. Lead-free solar cells based on tin halide perovskite films with high coverage and improved aggregation. *Angew. Chem., Int. Ed.* **2018**, *57*, 13221−13225.
(148) Li, L.; Wang, Y.; Wang, X.; Lin, R.; Luo, X.; Liu, Z.; Zhou, K.; Xiong, S.; Bao, Q.; Chen, G.; Tian, Y.; Deng, Y.; Xiao, K.; Wu, J.; Saidaminov, M. I.; Lin, H.; Ma, C.-Q.; Zhao, Z.; Wu, Y.; Zhang, L.; Tan, H. Flexible all-perovskite tandem solar cells approaching 25% efficiency with molecule-bridged hole-selective contact. *Nat. Energy* **2022**, *7*, 708−717.
(149) Jiang, W.; Li, F.; Li, M.; Qi, F.; Lin, F. R.; Jen, A. K. pi-expanded carbazoles as hole-selective self-assembled monolayers for high-performance perovskite solar cells. *Angew. Chem., Int. Ed.* **2022**, *61*, 202213560.
(150) Truong, M. A.; Funasaki, T.; Ueberricke, L.; Nojo, W.; Murdey, R.; Yamada, T.; Hu, S.; Akatsuka, A.; Sekiguchi, N.; Hira, S.; Xie, L.; Nakamura, T.; Shioya, N.; Kan, D.; Tsuji, Y.; Iikubo, S.; Yoshida, H.; Shimakawa, Y.; Hasegawa, T.; Kanemitsu, Y.; Suzuki, T.; Wakamiya, A. *J. Am. Chem. Soc.* **2023**, *145*, 7528.
(151) Zillner, J.; Boyen, H.-G.; Schulz, P.; Hanisch, J.; Gauquelin, N.; Verbeeck, J.; Küffner, J.; Desta, D.; Eisele, L.; Ahlswede, E.; Powalla, M. The role of $SnF_2$ additive on interface formation in all lead-free $FASnI_3$ perovskite solar cells. *Adv. Funct. Mater.* **2022**, *32*, 2109649.
(152) Warby, J.; Zu, F. S.; Zeiske, S.; Gutierrez-Partida, E.; Frohloff, L.; Kahmann, S.; Frohna, K.; Mosconi, E.; Radicchi, E.; Lang, F.; Shah, S.; Pena-Camargo, F.; Hempel, H.; Unold, T.; Koch, N.; Armin, A.; De Angelis, F.; Stranks, S. D.; Neher, D.; Stolterfoht, M. Understanding performance limiting interfacial recombination in pin perovskite solar cells. *Adv. Energy Mater.* **2022**, *12*, 2103567.


https://doi.org/10.1021/prechem.3c00018
*Precis. Chem.* 2023, 1, 69−82

(153) Li, B.; Wu, X.; Zhang, H.; Zhang, S. F.; Li, Z.; Gao, D. P.; Zhang, C. L.; Chen, M. Q.; Xiao, S.; Jen, A. K. Y.; Yang, S. F.; Zhu, Z. L. Efficient and stable tin perovskite solar cells by pyridine-functionalized fullerene with reduced interfacial energy loss. *Adv. Funct. Mater.* **2022**, *32*, 2205870.
(154) Sun, C.; Yang, P.; Nan, Z.; Tian, C.; Cai, Y.; Chen, J.; Qi, F.; Tian, H.; Xie, L.; Meng, L.; Wei, Z. Well-defined fullerene bisadducts enable high-performance tin-based perovskite solar cells. *Adv. Mater.* **2023**, *35*, 2205603.
(155) Yuan, J.; Zhang, C. J.; Qiu, B. B.; Liu, W.; So, S. K.; Mainville, M.; Leclerc, M.; Shoaee, S.; Neher, D.; Zou, Y. P. Effects of energetic disorder in bulk heterojunction organic solar cells. *Energy Environ. Sci.* **2022**, *15*, 2806−2818.
(156) Shao, Y. C.; Yuan, Y. B.; Huang, J. S. Correlation of energy disorder and open-circuit voltage in hybrid perovskite solar cells. *Nat. Energy* **2016**, *1*, 15001.
(157) Lin, Y.; Chen, B.; Zhao, F.; Zheng, X.; Deng, Y.; Shao, Y.; Fang, Y.; Bai, Y.; Wang, C.; Huang, J. Matching charge extraction contact for wide-bandgap perovskite solar cells. *Adv. Mater.* **2017**, *29*, 1700607.
(158) Liu, W.; Hu, S.; Pascual, J.; Murdey, R.; Wakamiya, A. Tin halide perovskite solar cells with open-circuit voltages approaching the Shockley-Queisser limit. Under review.
(159) Jiang, Y.; Wang, J.; Zai, H.; Ni, D.; Wang, J.; Xue, P.; Li, N.; Jia, B.; Lu, H.; Zhang, Y.; Wang, F.; Guo, Z.; Bi, Z.; Xie, H.; Wang, Q.; Ma, W.; Tu, Y.; Zhou, H.; Zhan, X. Reducing energy disorder in perovskite solar cells by chelation. *J. Am. Chem. Soc.* **2022**, *144*, 5400−5410.
(160) Wang, X.; Fan, Y.; Wang, L.; Chen, C.; Li, Z.; Liu, R.; Meng, H.; Shao, Z.; Du, X.; Zhang, H.; Cui, G.; Pang, S. Perovskite solution aging: What happened and how to inhibit? *Chem.* **2020**, *6*, 1369−1378.
(161) Hu, S.; Pascual, J.; Liu, W.; Funasaki, T.; Truong, M. A.; Hira, S.; Hashimoto, R.; Morishita, T.; Nakano, K.; Tajima, K.; Murdey, R.; Nakamura, T.; Wakamiya, A. A universal surface treatment for p-i-n perovskite solar cells. *ACS Appl. Mater. Interfaces* **2022**, *14*, 56290−56297.
(162) Chen, H.; Maxwell, A.; Li, C.; Teale, S.; Chen, B.; Zhu, T.; Ugur, E.; Harrison, G.; Grater, L.; Wang, J.; Wang, Z.; Zeng, L.; Park, S. M.; Chen, L.; Serles, P.; Awni, R. A.; Subedi, B.; Zheng, X.; Xiao, C.; Podraza, N. J.; Filleter, T.; Liu, C.; Yang, Y.; Luther, J. M.; De Wolf, S.; Kanatzidis, M. G.; Yan, Y.; Sargent, E. H. Regulating surface potential maximizes voltage in all-perovskite tandems. *Nature* **2023**, *613*, 676−681.
(163) Li, F.; Deng, X.; Qi, F.; Li, Z.; Liu, D.; Shen, D.; Qin, M.; Wu, S.; Lin, F.; Jang, S. H.; Zhang, J.; Lu, X.; Lei, D.; Lee, C. S.; Zhu, Z.; Jen, A. K. Regulating surface termination for efficient inverted perovskite solar cells with greater than 23% efficiency. *J. Am. Chem. Soc.* **2020**, *142*, 20134−20142.
(164) Kapil, G.; Bessho, T.; Maekawa, T.; Baranwal, A. K.; Zhang, Y.; Kamarudin, M. A.; Hirotani, D.; Shen, Q.; Segawa, H.; Hayase, S. Tin-lead perovskite fabricated via ethylenediamine interlayer guides to the solar cell efficiency of 21.74%. *Adv. Energy Mater.* **2021**, *11*, 2101069.
(165) Kamarudin, M. A.; Hirotani, D.; Wang, Z.; Hamada, K.; Nishimura, K.; Shen, Q.; Toyoda, T.; Iikubo, S.; Minemoto, T.; Yoshino, K.; Hayase, S. Suppression of charge carrier recombination in lead-free tin halide perovskite via Lewis base post-treatment. *J. Phys. Chem. Lett.* **2019**, *10*, 5277−5283.
(166) Menzel, D.; Al-Ashouri, A.; Tejada, A.; Levine, I.; Guerra, J. A.; Rech, B.; Albrecht, S.; Korte, L. Field effect passivation in perovskite solar cells by a LiF interlayer. *Adv. Energy Mater.* **2022**, *12*, 2201109.
(167) Taddei, M.; Smith, J. A.; Gallant, B. M.; Zhou, S. R.; Westbrook, R. J. E.; Shi, Y. W.; Wang, J.; Drysdale, J. N.; McCarthy, D. P.; Barlow, S.; Marder, S. R.; Snaith, H. J.; Ginger, D. S. Ethylenediamine addition improves performance and suppresses phase instabilities in mixed-halide perovskites. *ACS Energy Lett.* **2022**, *7*, 4265−4273.
(168) Hu, J. T.; Chen, P.; Luo, D. Y.; Dai, L. J.; Chen, N.; Li, S. D.; Yang, S. Y.; Fu, Z. W.; Wang, D. K.; Gong, Q. H.; Stranks, S. D.; Zhu, R.; Lu, Z. H. Anchoring of halogen-cleaved organic ligands on perovskite surfaces. *Energy Environ. Sci.* **2022**, *15*, 5340−5349.
(169) Ansari, F.; Shirzadi, E.; Salavati-Niasari, M.; LaGrange, T.; Nonomura, K.; Yum, J. H.; Sivula, K.; Zakeeruddin, S. M.; Nazeeruddin, M. K.; Gratzel, M.; Dyson, P. J.; Hagfeldt, A. Passivation mechanism exploiting surface dipoles affords high-performance perovskite solar cells. *J. Am. Chem. Soc.* **2020**, *142*, 11428−11433.
(170) Chen, Q.; Wang, C.; Li, Y.; Chen, L. Interfacial dipole in organic and perovskite solar cells. *J. Am. Chem. Soc.* **2020**, *142*, 18281−18292.
(171) Bai, S.; Da, P.; Li, C.; Wang, Z.; Yuan, Z.; Fu, F.; Kawecki, M.; Liu, X.; Sakai, N.; Wang, J. T.; Huettner, S.; Buecheler, S.; Fahlman, M.; Gao, F.; Snaith, H. J. Planar perovskite solar cells with long-term stability using ionic liquid additives. *Nature* **2019**, *571*, 245−250.
(172) Chen, S.; Xiao, X.; Chen, B.; Kelly, L. L.; Zhao, J.; Lin, Y.; Toney, M. F.; Huang, J. Crystallization in one-step solution deposition of perovskite films: Upward or downward? *Sci. Adv.* **2021**, *7*, eabb2412.
(173) Dessimoz, M.; Yoo, S. M.; Kanda, H.; Igci, C.; Kim, H.; Nazeeruddin, M. K. Phase-pure quasi-2D perovskite by protonation of neutral amine. *J. Phys. Chem. Lett.* **2021**, *12*, 11323−11329.
(174) Noel, N. K.; Wenger, B.; Habisreutinger, S. N.; Snaith, H. J. Utilizing nonpolar organic solvents for the deposition of metal-halide perovskite films and the realization of organic semiconductor/perovskite composite photovoltaics. *ACS Energy Lett.* **2022**, *7*, 1246−1254.
(175) Zhu, Z. J.; Mao, K. T.; Zhang, K.; Peng, W.; Zhang, J. Q.; Meng, H. G.; Cheng, S.; Li, T. Q.; Lin, H. Z.; Chen, Q.; Wu, X. J.; Xu, J. X. Correlating the perovskite/polymer multi-mode reactions with deep-level traps in perovskite solar cells. *Joule* **2022**, *6*, 2849−2868.
(176) Huang, Y.; Yan, K.; Niu, B.; Chen, Z.; Gu, E.; Liu, H.; Yan, B.; Yao, J.; Zhu, H.; Chen, H.; Li, C.-Z. Finite perovskite hierarchical structures via ligand confinement leading to efficient inverted perovskite solar cells. *Energy Environ. Sci.* **2023**, *16*, 557.
(177) Kirmani, A. R.; Ostrowski, D. P.; VanSant, K. T.; Byers, T. A.; Bramante, R. C.; Heinselman, K. N.; Tong, J.; Stevens, B.; Nemeth, W.; Zhu, K.; Sellers, I. R.; Rout, B.; Luther, J. M. Metal oxide barrier layers for terrestrial and space perovskite photovoltaics. *Nat. Energy* **2023**, *8*, 191−202.
(178) Swartwout, R.; Hoerantner, M. T.; Bulovic, V. Scalable deposition methods for large-area production of perovskite thin films. *Energy Environ. Mater.* **2019**, *2*, 119−145.
(179) Barden, J.; Powell, R. C. Vapor transport deposition method and system for material co-deposition. US 9,490,120 B2, 2016.
(180) Lopez-Garcia, J.; Ozkalay, E.; Kenny, R. P.; Pinero-Prieto, L.; Shaw, D.; Pavanello, D.; Sample, T. Implementation of the IEC TS 60904−1-2 measurement methods for bifacial silicon PV devices. *IEEE J. Photovolt.* **2022**, *12*, 787−797.
(181) Li, H.; Wang, Y.; Gao, H.; Zhang, M.; Lin, R.; Wu, P.; Xiao, K.; Tan, H. Revealing the output power potential of bifacial monolithic all-perovskite tandem solar cells. *eLight* **2022**, *2*, 21.
(182) Gil-Escrig, L.; Hu, S.; Zanoni, K. P. S.; Paliwal, A.; Hernandez-Fenollosa, M. A.; Roldan-Carmona, C.; Sessolo, M.; Wakamiya, A.; Bolink, H. J. Perovskite/perovskite tandem solar cells in the substrate configuration with potential for bifacial operation. *ACS Mater. Lett.* **2022**, *4*, 2638−2644.